

5-2017

Characterizing the source of neutrophil elastase and proteinase 3 cross-presentation in B-cell acute lymphoblastic leukemia

Selena Carmona

Follow this and additional works at: https://digitalcommons.library.tmc.edu/utgsbs_dissertations



Part of the [Medicine and Health Sciences Commons](#)

Recommended Citation

Carmona, Selena, "Characterizing the source of neutrophil elastase and proteinase 3 cross-presentation in B-cell acute lymphoblastic leukemia" (2017). *The University of Texas MD Anderson Cancer Center UTHealth Graduate School of Biomedical Sciences Dissertations and Theses (Open Access)*. 751.
https://digitalcommons.library.tmc.edu/utgsbs_dissertations/751

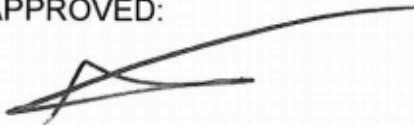
This Thesis (MS) is brought to you for free and open access by the The University of Texas MD Anderson Cancer Center UTHealth Graduate School of Biomedical Sciences at DigitalCommons@TMC. It has been accepted for inclusion in The University of Texas MD Anderson Cancer Center UTHealth Graduate School of Biomedical Sciences Dissertations and Theses (Open Access) by an authorized administrator of DigitalCommons@TMC. For more information, please contact digitalcommons@library.tmc.edu.

CHARACTERIZING THE SOURCE OF NEUTROPHIL ELASTASE AND
PROTEINASE-3 CROSS-PRESENTATION IN B-CELL ACUTE LYMPHOBLASTIC
LEUKEMIA

By

Selena Nicole Carmona, B.S

APPROVED:



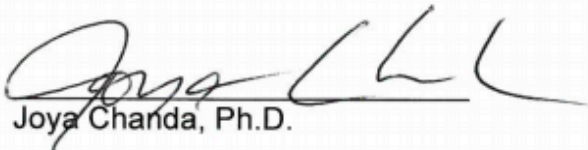
Gheath, Al-Atrash, DO, Ph.D, Advisory Professor



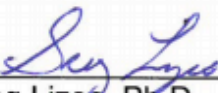
Jeff Molldrem, MD, Advisory Professor



Dean Lee, MD, Ph.D.



Joya Chanda, Ph.D.



Greg Lizee, Ph.D.

APPROVED:

Dean, The University of Texas
MD Anderson Cancer Center UTHealth Graduate School of Biomedical Sciences

CHARACTERIZING THE SOURCE OF NEUTROPHIL ELASTASE AND
PROTEINASE-3 CROSS-PRESENTATION IN B-CELL ACUTE LYMPHOBLASTIC
LEUKEMIA

A
THESIS

Presented to the Faculty of
The University of Texas
MD Anderson Cancer Center UTHealth
Graduate School of Biomedical Sciences

In Partial Fulfillment
Of the Requirements
For the Degree of
MASTER OF SCIENCE

By
Selena Nicole Carmona, B.S.

Houston, Texas

May 2017

Dedication

This work is dedicated to my loving husband, Sebastian Carmona, who has always supported me in all my hopes and dreams.

Acknowledgements

I would first like to thank my advisors, Dr. Gheath Al-Atrash and Dr. Jeffrey Molldrem, for their scientific and professional guidance throughout my training in their lab. I can truly say that my growth as a scientist is owed to them. I would also like to thank my supervisory committee, Drs. Dean Lee, Joya Chandra, and Greg Lizée, for their insight and input on the progression of my project. All have been crucial in my development as a scientist in these past few years. I would also like to thank all members of the Al-Atrash, Molldrem, and Mittendorf labs. Not only have they made the lab a great place to work, but the numerous scientific discussions, constant advice and patience were always so helpful. Specifically, Drs. Elizabeth Mittendorf, Lisa St. John, Celine Kerros, Anne Phillips, Mao Zhang, Na Qiao, Haley Peters, Haven Garber, and Anna Seergeva along with Pariya Sukhumalchandra, and Alex Perakis. All have helped greatly in the development of protocols, trouble-shooting, advice and analysis of data. Another intricate part of my work is all members of the South Campus Flow Core Facility including Dr. Karen Clise-Dwyer and her entire team. With flow-cytometry being an important aspect of my project, all members of the Flow Core Facility have helped in the planning of experiments and the analysis of data. My work would not have been possible if not for these three groups of scientists.

Lastly, I owe a great amount of gratitude to those that have always supported me throughout my graduate school career. My family, including my mom, Cynthia Zaldivar and my sisters, Stefany Hernandez, Christina Spooner and Grace Moon, have always supported my career choices and believed in me. More importantly, my husband, Sebastian Carmona, for always reading my papers, picking up the slack, and being there for me when things did not go as planned. For that, I will always be grateful.

CHARACTERIZING THE SOURCE OF NEUTROPHIL ELASTASE AND PROTEINASE 3 CROSS PRESENTATION IN ACUTE LYMPHOBLASTIC LEUKEMIA

Selena Nicole Carmona, B.S.

Advisory Professors: Gheath Al-Atrash, DO, Ph.D./Jeffrey Molldrem, MD

Discovery of tumor-associated antigens is an important step in designing effective antigen-targeting immunotherapies. PR1 is a nonameric human leukocyte antigen (HLA)-A2 restricted leukemia-associated antigen derived from serine proteases neutrophil elastase (NE) and proteinase 3 (P3). NE and P3 are primarily expressed in cells of myeloid lineage including granulocytes, bone marrow progenitors and myeloid leukemia. Our lab reported that NE and P3 are cross-presented by antigen presenting cells (APCs) and solid tumors, a mechanism whereby exogenous antigens are endocytosed and presented on HLA class I molecules, inducing a cytotoxic T lymphocyte (CTL)-mediated immune response. Therefore, identifying non-myeloid tumors capable of PR1 cross-presentation broadens the application of PR1-targeted immunotherapies, which to date include PR1 peptide vaccine¹, PR1 cellular therapy^{2,3} and 8F4, a T cell receptor (TCR)-like monoclonal antibody (mAb)^{4,5}.

One possible source of NE and P3 in the microenvironment is neutrophil extracellular traps (NETs). NETs are composed of deoxyribonucleic acid (DNA)/histones extruded from polymorphonuclear neutrophils (PMNs) abundant in antimicrobial proteases, including NE and P3. Although a main function of NETs is elimination of pathogens, seminal studies have demonstrated immune-regulatory effects of NETs. Thus there lies a great interest in understanding the role of NETs in modulating adaptive immune system through cross-priming or cross-tolerance in the setting of anti-tumor immunity. We are specifically interested in possible roles of NETs

in facilitating NE and P3 cross-presentation by acute lymphoblastic leukemia (ALL) due to its high abundance in the bone marrow.

The major aim of this study was to validate PR1 as a target in B-ALL. This hypothesis is based on strong data from our laboratory showing (1) uptake and cross-presentation of NE and P3 by APCs^{6,7} including B cells, and (2) susceptibility of non-myeloid tumors to killing by 8F4 and PR1-CTLs (PR1-specific cytotoxic T lymphocytes) following PR1 cross-presentation⁶. Knowledge gained will define PR1 as a therapeutic target and cross-presentation as a mechanism for antigen expression in B-ALL.

My results identify PR1 as a target in B cell-ALL, and identify NETs as a source of NE and P3 in the tumor microenvironment. These findings implicate the use of PR1-targeting immunotherapies as a novel form of treatment in B cell-ALL.

Table of Contents

Approval Page.....	i
Title Page	ii
Dedication	iii
Acknowledgements	iv
Abstract.....	v
Table of Contents	vii
List of Illustrations.....	x
List of Tables	xii
Abbreviations.....	xiii
Chapter One: Introduction	1
1.1 Leukemia	1
1.1.1 B Cell Lymphoblastic Leukemias	1
1.1.2 Allogeneic Stem Cell Transplantation in Leukemia.....	3
1.1.3 NE, P3, and PR1	4
1.1.4 8F4	7
1.2 Antigen Presentation	8
1.3 NETs, abundant in NE and P3, serve as a possible source in the tumor microenvironment	11
1.4 Project Summary and Hypothesis	12
Chapter 2: Materials and Methods	14
2.1 Cell Lines	14

2.2 HLA-A2 Transduction	16
2.3 Generation of Protein Lysates and Western Blots.....	17
2.4 RNA Purification and RT-PCR.....	18
2.5 NE and P3 uptake in B-ALL cell lines	19
2.6 PR1 Cross-Presentation	20
2.7 PR1-specific CTLs	21
2.8 PR1-CTL Cytotoxicity Assay.....	22
2.9 Induction of NET formation and identification via flow cytometry	22
2.10 Identification of NETs via confocal microscopy	23
2.11 Determine whether NETs are a source of NE and P3 uptake	24
Chapter Three: Results	26
3.1 B-ALL cell lines cross-present PR1 rendering them susceptible to killing by PR1- targeting immunotherapy	26
3.1.1 B-ALL cell lines Lack Intracellular Expression of NE and P3	26
3.1.2 B-ALL cell lines take up soluble and PMN-associated NE and P3	27
3.1.3 P3 is taken up at a greater extent than NE in B-ALL cell lines.....	34
3.1.4 Endogenous HLA-A2 surface expression in B-ALL cell lines.....	40
3.1.5 NE and P3 are cross-presented by B-ALL cell lines	40
3.1.6 PR1 cross-presentation renders B-ALL cell line susceptible to PR1-CTLs...	42
3.2 NETs serve as a possible source of NE and P3 uptake in B-ALL cell lines	45
3.2.1 Identification of NET-inducing PMNs via flow cytometry	45
3.2.2 Identification of NET-inducing PMNs via confocal microscopy	46
3.2.3 NET-associated NE and P3 are taken up by B-ALL cell lines.....	46
Chapter Four: Discussion and Future Direction	57

4.1 Discussion	57
4.2 Future Directions	69
References	73
Vita	89

List of Illustrations

Figure 1: B-ALL cell line lack endogenous expression of NE	27
Figure 2: B-ALL cell lines lack endogenous expression of P3	28
Figure 3: B-ALL cell lines take up soluble NE and P3.....	29
Figure 4: Intracellular uptake of NE and P3 occurs in B-ALL cell lines	31
Figure 5: Uptake of soluble NE and P3 plateaus over time in B-ALL cell lines	32
Figure 6: PMN-associated NE is taken up in B-ALL cell lines.....	34
Figure 7: PMN-associated P3 it taken up in B-ALL cell lines	36
Figure 8: Soluble and PMN-associated P3 is taken up at a greater extent than soluble and PMN associated NE	38
Figure 9: Nalm6 and SB B-ALL cell lines are endogenously HLA-A2 positive.....	40
Figure 10: Cross-presentation of soluble NE and P3 increase B-ALL susceptibility to killing by PR1-CTLs.....	43
Figure 11: PMA and ionomycin induce NET formation in healthy PMNs, ionomycin at a greater extent	46
Figure 12: PMNs treated with ionomycin undergo NETosis.....	47
Figure 13: NET-associated NE is taken up in B-ALL cell lines.....	50
Figure 14: NET-associated P3 it taken up in B-ALL cell lines	51
Figure 15: DNase treatment inhibits NE uptake in B-ALL cell lines in a dose-dependent manner	52

Figure 16: DNase nor ionomycin have any effect on PMN-associated NE uptake in B-ALL cell lines	53
Figure 17: DNase nor ionomycin have any effect on PMN-associated P3 uptake in B-ALL cell lines	54
Figure 18: Resting and irradiated PMNs do not undergo NETosis without stimulation.	55
Figure 19: Proposed model of uptake and cross-presentation of NE and P3 renders B-ALL cell lines susceptible to killing by PR1-CRLS, PR1 vaccine and 8F4 mAb.....	68

List of Tables

Table 1: B-ALL Cell Line Phenotype	15
Table 2: Uptake of PMN-associated versus soluble NE in B-ALL cell lines	36
Table 3: Uptake of PMN versus soluble P3 in B-ALL cell lines	38

Abbreviations

ADCC = antibody dependent cytotoxicity assay

AF = Alexa Fluor

ALL = Acute Lymphoblastic Leukemia

ANCA = antineutrophil cytoplasmic antibodies

APC = Antigen Presenting Cell

APM = Antigen Presentation Machinery

BCR = B cell receptor

BME = β -mercaptoethanol

CTL = Cytotoxic T Lymphocyte

CTLA4 = cytotoxic T-lymphocyte-associated protein 4

DAMP = danger associated molecular pattern

DC = dendritic cell

DMSO = dimethyl sulfoxide

DNA = deoxyribonucleic acid

ER = endoplasmic reticulum

GM-CSF = granulocyte macrophage colony-stimulating factor

GPA = granulomatosis with polyangiitis

GvHD = Graft versus host disease

GvL = Graft versus Leukemia

H3Cit = histone 3 citrullination

HLA = Human Leukocyte Antigen

HSC = hematopoietic stem cell

IL = interleukin

LAA = leukemia-associated antigen

LSC = leukemia stem cell

mAb = monoclonal antibody

mDC = myeloid dendritic cells

MFI = median fluorescence intensity

MM = multiple myeloma

MPO = myeloperoxidase

NE = Neutrophil Elastase

NET = Neutrophil Extracellular Traps

P3 = Proteinase 3

PAR = protease-activated receptors

PBS = phosphate-buffered saline

PD1 = programmed death 1

PD-L1 = programmed death ligand 1

PMN = polymorphonuclear neutrophils

PR1-CTL = PR1-specific cytotoxic T lymphocyte

PVDF = polyvinylidene difluoride

TAP = transporter involved in antigen processing

TCR = T-cell Receptor

TNF = tumor necrosis factor

Tregs = regulatory T cells

Chapter One: Introduction

1.1 Leukemia

Leukemia is cancer of the bone marrow and lymphatic system and is defined by an accumulation of abnormal white blood cells and a lack of normal functionality. The result is the suppression of the development of healthy hematopoietic cells, and the production of a high number of immature and abnormal leukocytes. Leukemias can be broadly categorized into four types: ALL, chronic lymphocytic leukemia (CLL), acute myeloid leukemia (AML) and chronic myeloid leukemia (CML). There has been major progress in treatment of CML and CLL, which are generally chronic malignancies with good prognosis. However, there remains a desperate need for novel therapies for AML and ALL, especially in relapsed cases, as they are typically more aggressive.

1.1.1 B Cell Lymphoblastic Leukemias

ALL is a B or T cell precursor stage lymphoid malignancy where the differentiation process is inhibited by genetic alterations and the enhanced survival and proliferation of malignant cells⁸. B- cell ALL accounts for approximately 80% of ALL cases, the other 20% originating from T cell lineage⁹. Further, it accounts for approximately 80% of pediatric leukemias making it the most common pediatric hematologic malignancy, and 20% of adult leukemia cases.

ALL originates from the stem cells in the bone marrow and has the ability to spread to other areas as the central nervous system, the lymph nodes, the spleen and the testes. Blasts are produced when malignant cells become leukemic and begin to multiply uncontrollably. Leukemia lymphoblasts will then grow and survive at a rate

more efficient than normal cells. It is estimated that a total on 7000 people in the US were be diagnosed with ALL in 2016 with a median age of diagnosis at 15 and a 5 year survival rate of 68.1%, based on data from the National Cancer Institute.

ALL can start in either early B or T cells at different stages of maturity. B cell-ALL has four main subtypes including early pre B-ALL, common, pro B and mature B-ALL. Many prognostic factors can determine the survival of a patient, including age, initial white blood cell count, subtype, and presence of a chromosome abnormality, response to chemotherapy and status of the ALL treatment. Treatment typically occurs in three phases: induction, consolidation and maintenance. Total treatment is approximately 2 years long and treatment intensity depends on the subtype of ALL and previously mentioned prognostic factors. Though most ALL cases occur in children, four out of five deaths from ALL occur in adults indicative of a better prognosis in children. This difference occurs because children respond better to treatment, either due to a difference in the disease itself or because children are able to withstand more aggressive treatment.

The current treatment for ALL is Hyper-CVAD, a regimen that includes cyclophosphamide, vincristine sulfate, doxorubicin hydrochloride and dexamethasone. Cyclophosphamide is an alkylating agent that is most active in the resting phase of cells, and is therefore cell cycle non-specific. Vincristine sulfate is a plant alkaloid that is cell cycle specific. It is an agent that inhibits the microtubule structure within the cell, resulting in cell death. Doxorubicin hydrochloride intercalates between base pairs in the DNA helix, preventing DNA replication and inhibiting protein synthesis. Dexamethasone is an anti-inflammatory medication classified as a corticosteroid that is used to decrease swelling associated with tumors of the spine and brain. Although 80% of

patients respond to initial therapy, a number of patients fail to respond or relapse and are offered allogeneic stem cell transplantation. This is the only current curative treatment for relapsed and aggressive forms of ALL, highlighting the role of the immune system in eliminating ALL and the need to further develop therapies, which is the subject of my research.

1.1.2 Allogeneic Stem Cell Transplantation in Leukemia

Although my work focuses on B-ALL, the foundation for the immunotherapy that I have studied, i.e. PR1-targeting immunotherapy was initially based on targeting myeloid leukemia. The two main types of myeloid leukemia include chronic (CML) and acute (AML). CML is characterized by the accumulation of a high number of mature myeloid cells in the bone marrow while AML is characterized by the accumulation of immature blasts in the bone marrow, and has a much more aggressive course of treatment than CML.

Since the advent of tyrosine kinase inhibitors, CML has been rendered as a chronic disease in the majority of cases, with a 5-year survival of 65%, while the prognosis of AML remains dismal with a 5-year survival rate of 27%. However, there are very few effective treatment options for AML. Current forms of treatment include chemotherapy and allogeneic stem cell transplantation, a robust form of immunotherapy that is offered to myeloid leukemia patients who have poor prognostic factors. In fact, myeloid leukemias are the quintessential immunotherapy-sensitive tumors, as indicated by the cures that are achieved following allogeneic (allo) hematopoietic stem cell transplantation (HSCT) ¹⁰. Although allo-HSCT replenishes the hematopoietic components that are ablated following pre-allo-HSCT chemotherapy/radiation that the patient receives, donor derived T cells within the allo-

HSCT graft provide a potent immune response that targets the leukemia cells, hence providing the immunotherapeutic effect of the graft. However, allo-HSCT is associated with high toxicity and frequent occurrence of graft versus host disease (GvHD). This occurs in approximately 70% of patients making GvHD the leading cause of treatment-related mortality following allo-HSCT ¹¹.

Targeting individual antigens for immunotherapy has shown promising effects on tumor growth with less toxicity compared to allo-HSCT¹². This approach facilitates the elimination of malignant clones through the graft versus leukemia (GvL) effect while sparing normal tissue from the off-target effects of GvHD. One approach is to identify and target leukemia associated antigens (LAA). Tumor specific antigens have proven to be quite rare. However, a related concept involves targeting LAA. Derived from proteins expressed in normal tissue, they have an increased/aberrant expression in leukemia. Studies in our lab have identified the LAA PR1, a nonameric peptide derived from NE and P3, which will be discussed in detail in the following section.

1.1.3 NE, P3, and PR1

NE and P3 are serine proteases stored in neutrophil cytoplasmic azurophilic granules. Located on the terminal region of the short arm of chromosome 19, NE and P3 transcription occurs during the promyelocytic stage of neutrophil maturation¹³. Both play a large role in anti-microbial defense ¹⁴ and are endogenously expressed in granulocytes, monocytes, mast cells, and bone marrow myeloid progenitors. Both are also aberrantly expressed in AML and CML ¹⁵⁻¹⁷. Serine proteases function to digest and clear phagocytosed antigens in PMNs¹³. Although much of their cytotoxic function occurs within the neutrophil, NE and P3 are capable of being secreted once neutrophils are activated at sites of inflammation. Inflammatory stimulation initiates the

translocation of neutrophil granules to the plasma membrane wherein their contents are released into the microenvironment¹³. A portion remains bound to the PMN membrane in their active form so that chemokine, cytokine, growth factor and cell surface receptor functions can be regulated by both soluble and membrane-bound protease¹³. Further, one of many extracellular functions includes activating lymphocytes and the cleaving of adhesion molecules¹³. All of these functions identified the role of NE and P3 in both pro- and anti-inflammatory activities along with the effect on various immune responses at site of inflammation.

P3 has been associated with autoimmune diseases, including vasculitis and rheumatoid arthritis, when expressed on the neutrophil surface. Further, P3 is a target of antineutrophil cytoplasmic antibodies (ANCA) in granulomatosis with polyangiitis (GPA); formally known as Wegener granulomatosis, which is found in more than 80% of GPA patients. This is caused by P3 secretion from neutrophils that favors the development and progression of chronic inflammatory diseases. Although P3 had been identified in the aforementioned autoimmune diseases, it was important to determine how autoreactivity to antigens was initiated and whether the targeted autoantigens, in this case P3, played a role in the reversal of tolerance. Ludewig et al. identified that DCs in animal models played an important role in initiating and maintaining immune responses to self-antigen in autoimmune disease¹⁸. Therefore, Csernok et al. investigated the effect of P3 on immature DCs in patients with GPA, Crohn's disease, and other granulomatous diseases¹⁹. They reported that P3 induced DC maturation through induction of protease-activated receptor (PAR)-2 expression on immature DCs, and PAR-2 cleavage and activation. This was hypothesized based on data identifying the contribution of PAR expression to inflammation, high expression on DCs, and

activation of epithelial cells through PAR binding to P3. The cleaving of PAR-2 by P3 resulted in the induction of DCs to become functional APCs through up-regulation of CD83, CD86, CD83 and HLA-DR surface expression, along with the down-regulation of CD14, a molecule expressed by immature DCs. Mature DCs exposed to P3 acquired the ability to stimulate P3-specific CD4⁺ T cells, which produced IFN and had a Th1 phenotype. Expression of IFN favors the development of a granulomatosis inflammation as seen in GPA. This characterizes the role of P3 and PAR-2 in the induction of adaptive immunity and the reversal of tolerance in P3-targeting autoimmunity.

Derived from NE and P3, PR1 is a nonameric HLA-A2 restricted peptide. Immunity against PR1 was demonstrated in 2000 when our lab identified the importance of PR1 peptide in CTL immune responses against CML ¹⁷. Data identified the importance of targeting PR1 based its role in remission post transplant.

The identification of tumor associated antigens, such as PR1, and the design of tetramers to identify peptide/MHC allows the ability to detect tumor antigen-specific T cell responses. CTLs identified that selectively target PR1 have been shown to be elevated in myeloid leukemia patients ⁷ and have cytotoxic function against malignant cells along with the inhibition of progenitor cell growth ^{20,21}. Their cytotoxic function has also been shown to greatly contribute to cytogenetic and molecular remission of CML patients treated with interferon-alpha or allogeneic stem cell transplant¹⁷. This suggested that interferon treatment induced remission through the expansion of autologous PR1-CTLs ¹⁷. A possible mechanism of action was identified as the up regulation of MHC class I or tumor antigen on malignant cells resulting in a robust CTL response ¹⁷. A second method of action includes the strong GvL effect post transplant

so that allogeneic CTL target self-peptide on malignant cells ¹⁷. The successful killing of chronic and acute myeloid leukemia cells by PR1-CTLs supports the targeting of surface PR1-CTLs to elicit an immune response and the boosting of anti-leukemia responses.

As previously described, the GvL effect following allogeneic stem-cell transplantation was quite robust in eliminating malignant cells. Therefore, identifying a form of treatment that boosts immunity against PR1 may prove to be beneficial for treatment of myeloid leukemias. A peptide vaccine was identified to induce and enhance leukemia-specific T cell responses to PR1²². This response was robust due to a higher frequency of PR1-specific CD8+ T cells with a memory phenotype in patients with leukemia in comparison to healthy individuals ^{17,21,23}. Studies also showed that post vaccine administration there was a reduction in leukemia burden indicative of an immune response against MDS and leukemia ²². These results validated targeting of endogenous peptides, such as PR1, with various forms of immunotherapy including vaccination and adoptive cell therapy in combination with current forms of treatment.

A newer form of treatment against tumor-specific antigens includes monoclonal antibodies (mAb). mAb used in clinical settings target surface proteins that are expressed on normal cells yet are overexpressed in malignant cells ^{4,5} and have an increased effectiveness due to the ease and ability of frequent dosage. A mAb engineered in our lab called 8F4 will be discussed in the subsequent section.

1.1.4 8F4

The significance of PR1-targeting immunotherapy was highlighted through two main observations: PR1-CTLs contributed to remission in myeloid leukemia patients treated with interferon and allogeneic stem cell transplant ^{17,24}, and PR1 vaccination

induced a robust CD8 response in myeloid malignancies^{1,25}. However, because tumor burden is a limiting step in immunotherapy, our group developed an anti-PR1/HLA-A2 mAb, 8F4, that can overcome high disease burden through repeat high-dose administration⁴. There also exists a need to target chemo-resistant leukemia stem cells (LSC) as relapse rates are quite high. A therapeutic advantage of TCR-like mAb includes the increased affinity binding to surface peptide/MHC complexes²⁶⁻³⁰ compared to the very low affinity of a TCR^{31,32}. 8F4 is a TCR-like IgG2a mAb that binds the combined epitope of the PR1/HLA-A2 with very high affinity⁴. Studies showed that 8F4 has success in mediating complement-dependent cytotoxicity (CDC) of AML but not normal leukocytes. Further data showed the inhibition in the growth of AML progenitor cells, and the lysis of LSC, but no effect on normal progenitors from healthy donors⁴. Further 8F4 reduced tumor burden in relapsed, refractory, and secondary AML identifying its efficacy in aggressive forms of leukemia⁵.

Despite success in current treatment in inducing remission, relapse rates are quite high. This is attributed to LSC that are not affected by chemotherapy. Therefore, the ability of 8F4 to induce lysis of LSCs and secondary AML warrants the broadening of TCR-like antibody development to target other leukemia-associated peptide/MHC complexes.

1.2 Antigen Presentation

The biggest hurdle for developing effective immunotherapies is in identifying tumor antigen. To induce a T cell response against antigen, the target cell must express it. MHC class I molecules, expressed on nearly all somatic cells, typically bind *intracellular* peptides and are recognized by CD8 T cells inducing a cytotoxic response when expressed on the cell surface. This process begins when proteins are degraded

via cytosolic and nuclear proteins and result in peptides approximately 8-16 amino acids long. Peptides are then bound to the MHC class I molecule forming a stable complex. Once this occurs, peptide/MHC-I is transported to the cell surface wherein CD8 T cells will recognize the peptide complex through its TCR. Then with secondary signaling from co-stimulatory and co-inhibitory receptors, T cells are activated and lyse the target cell. MHC class II antigen presentation on the other hand includes the uptake of *exogenous* antigen and is therein recognized by CD4 helper T cells on the cell surface of APC, specifically dendritic cells (DCs) or B cells. MHC class I is involved in eliciting cytotoxic T cell response whereas MHC class II antigen presentation is involved in CD4 helper T cell and B cell response.

Cross-presentation is another mechanism that activates naïve CD8 T cells targeting extracellular antigens. Through this mechanism, antigens are taken up and presented on MHC class I molecules to elicit a CD8 T cell response³³. Most studies to date in which cross-presentation of tumor derived antigen occurs focused on APCs, and the ability of tumors to evade the immune system through the down regulation of antigen presentation³⁴. However, a more recent study identified the ability of non-APCs, in this case mesenchymal stromal cells, to cross-present tumor antigen³⁵ highlighting the importance of antigen cross-presentation in eliciting anti-tumor immunity.

As previously mentioned, PR1 is targeted in myeloid leukemia through PR1 vaccine^{1,25}, PR1-CTLs^{17,20}, and 8F4 mAb^{4,5}. We broadened this to other tumors, such as breast cancer, that can have monocytic and neutrophilic infiltration, and therefore the presence of NE and P3. Although NE and P3 are primarily expressed in hematopoietic cells of the myeloid lineage, studies reported NE and P3 in breast

cancer tissue³⁶⁻³⁸. The source of NE was unknown but endogenous expression was identified in breast cancer cells^{39,40}. We were unable to confirm endogenous expression in breast cancer cell lines ourselves, so we hypothesized that intracellular expression of NE and P3 in breast cancer was due to uptake. Because some breast cancer subtypes are known to have PMN and monocyte infiltrations⁴¹ that release NE and P3 into the microenvironment, our lab tested whether PMNs serve as a source of NE and P3 uptake in breast cancer. Our lab confirmed uptake of both soluble and PMN-associated NE and P3 in breast cancer cell lines that lack endogenous NE and P3 with increasing uptake over time^{6,42}. After uptake, PR1, a peptide derived from NE and P3, was shown to be cross-presented in HLA-A2+ breast cancer cells lines following NE and P3 uptake at 24 hours^{6,42}. Because PR1 can be successfully targeted in myeloid leukemias, our lab confirmed the broadening of PR1-targeted therapies by identifying the killing of breast cancer cell lines after PR1 cross-presentation by PR1-CTLs and 8F4 Ab^{6,42}. This phenomenon was further shown in lung cancer, a tumor also characterized by possible neutrophilic and monocytic infiltration⁴³. Our study provided evidence that cross-presentation is a novel mechanism whereby hematopoietic antigens are expressed on solid tumors.

Previous studies from our lab have also shown that normal and leukemic APCs, including B cells, cross-present PR1⁷. This was the basis of my thesis in studying the ability of B-ALL to cross-present PR1. This hypothesis is furthered strengthened by the location of B-ALL in the bone marrow, as this is an area rich in NE and P3. The bone marrow is also present with inflammatory cells such as PMNs and monocytes, cells that routinely secrete NE and P3. This set the basis of my project in further identifying the susceptibility of non-myeloid tumors to killing by PR1-targeting immunotherapies.

Although neutrophils are abundant in the microenvironment and infiltrate various tumor types, the mechanism of NE and P3 uptake by tumor cells remains poorly understood. NETs, abundant in NE and P3, are the result of a unique form of cell death that allows neutrophil granule contents to be released into the microenvironment. We therefore hypothesized that NETs serve as a possible source of protease uptake. This will be discussed further in the subsequent section.

1.3 NETs, abundant in NE and P3, serve as a possible source in the tumor microenvironment

NE and P3, proteases secreted by PMNs in the microenvironment, have an additional extracellular mechanism by which they have antimicrobial effects¹³. This cytotoxic effect lies in the formation of NETs: DNA secreted by activated neutrophils abundant in histones and various neutrophil serine proteases. NETs, a result of a unique form of neutrophil-programmed cell death, are characterized by a loss of intracellular membranes followed by the rupture of the cytoplasmic membrane. As previously mentioned, NETs are composed of DNA, histones, and various antimicrobial proteases, including NE, P3, myeloperoxidase (MPO), Cathepsin G, and various others. This form of cell death is independent of apoptosis and necrosis but is still considered a form of antimicrobial cell death⁴⁴.

Previous studies showed that PMNs, and more specifically NETs, have a large role in anticancer immunity and autoimmunity, specifically, in patients with ANCA-related autoimmunity and systemic lupus erythematosus (SLE)⁴⁵. Sangaletti et al. confirmed a direct correlation among the formation of NETs and the production of ANCA, which target neutrophilic intracellular proteins MPO and P3. Therefore, the

break in tolerance toward neutrophilic cytoplasmic proteins implied their necessary availability in the microenvironment to be presented on the surface of APCs for recognition⁴⁵. This identified apoptotic neutrophils as a source of neutrophil auto antigens. However, in PMNs undergoing necrosis, cytoplasmic granules undergo structural changes that alter MPO and P3 epitope confirmation making them unable to be cross-presented by APCs⁴⁵. On the other hand, in NETosing PMNs, cytoplasmic proteins are associated with nucleic acid and histones maintaining their conformation, their antimicrobial function and the ability to be cross-presented⁴⁵. In this study, data confirmed that NETs have the ability to transfer neutrophil cytoplasmic proteins to mDCs resulting in cross-presentation that trigger an adaptive immune response as indicated by ANCA production. In identifying the ability of NETs to serve as a source of cytoplasmic neutrophilic proteins that are enzymatically active in the microenvironment, we therefore hypothesized that NETs are capable of transferring NE and P3 to B-ALL cell lines inducing PR1 cross-presentation.

1.4 Project Summary and Hypothesis

Due to our success in PR1 targeting on myeloid leukemia and solid tumors, the presence of NE and P3 in the bone marrow microenvironment and the ability of APCs, including B cells, to cross-present PR1, we hypothesized that the lymphoid malignancy B-ALL takes up and cross presents NE and P3 from the bone marrow microenvironment. This further broadens the use of accepted PR1 targeting therapies including PR1-CTLs, PR1 vaccine and 8F4 mAb, to tumors with possible neutrophilic and monocytic infiltration.

In this study, we evaluated whether 1) B-ALL cell lines cross-present PR1; 2) whether PR1-targeting immunotherapies effectively target B-cell ALL; and 3) whether

NETs are a source of NE and P3 uptake. We provided data that ALL cell lines take up soluble and PMN-associated NE and P3, and cross-present PR1 from both sources. Further, we confirmed NETs serve as a source of NE and P3 uptake, however are not as efficient as resting PMNs as a source. Together our data demonstrated PR1 cross-presentation in B cell ALL and its targeting by PR1-CTLs.

Chapter 2: Materials and Methods

2.1 Cell Lines

Healthy-donor peripheral blood mononuclear cells (PBMC) and PMN were isolated from buffy coats obtained from Gulf Coast Blood Bank by single or double Ficoll gradient using Histopaque-1077 and Histopaque-1119 (Sigma Aldrich). SupB15 (B lymphoblast leukemia), SB (B lymphoblast leukemia), and T2 (B cell/T cell hybridoma) cell lines were obtained from American Type Culture Collection (ATCC). RS4 (B lymphoblastic leukemia) and Nalm6 (B lymphoblastic leukemia) cell lines were kindly provided by Dr. Dean Lee (Ohio State University). Cells were cultured in RPMI 1640 media with 2.5 mM L-glutamine (Hyclone) supplemented with 10% fetal bovine serum, 100 U/mL penicillin, and 100 µg/mL streptavidin (Invitrogen). All cells were grown in a humidified incubator set at 37 °C and 5% CO₂. Cells lines were validated at the MD Anderson Sequencing and Microarray Facility using short tandem repeat DNA fingerprinting and checked for mycoplasma on a routine basis via PCR (PromoKine). Surface phenotype of each cell line was determined by flow cytometry. Standard B-cell markers (anti-human-CD19-PE, anti-human CD10-BV421, anti-human C34-Pe/Cy7, anti-human CD38-AF700 antibodies all obtained from BioLegend) were incubated with cells at a 1:50 dilution for 30 minutes on ice. Phenotype of each cell line is listed below in Table 1

Table 1: B-ALL Cell Line Phenotype

Cell Line	CD19	CD34	CD10	CD38
RS4	Positive	Negative	Negative	Positive
SB	Positive	Negative	Negative	Positive
Supb15	Positive	Positive	Positive	Negative
Nalm6	Positive	Positive	Negative	Negative

2.2 HLA-A2 Transduction

HLA-A2*0201 transfection was done using lentiviral vectors as previously described ⁴⁶. The first step included packaging the lentivirus with the use of 293METR cells. The 239METR cells were thawed and grown in dMEM media (HyClone) with 10% fetal bovine serum (FBS) (Gemini Bio-Products, Sacramento, CA, USA) to 90% confluency in a T150 flask. Cells are then seeded in a T150 flask at 4.5×10^6 cells per total volume forty-eight hours prior to transfection or 1.125×10^7 cells twenty-four hours prior transfection. Viruses were collected 48 hours and 72 hours after transfection. Each transfection reaction requires 2 μ g VSV g plasmid, 4.7 μ g pCMV R8.2 or R8.91 plasmid and 2.3 μ g Lentiviral vector. In a 15 mL tube, the plasmid, pCMV R8.9 and Lentiviral vector were combined in 4.5 mL of Opti-MEM media and incubated at room temperature for 5 minutes. In a second 15 mL tube, 90 μ L LipofectAmine 2000 and 4.5 mL of Opti-MEM media (Gibco) were combined and incubated at similar incubation conditions. Tubes 1 and 2 were then combined and incubated at room temperature for 30 minutes.

In T150 flasks with confluent 293-METR cells, 6 mL of Opti-MEM media were added along with the 9 mL of Tube 1 and 2. Five hours post transfection, the virus was aspirated and fresh 20 mL dMEM with 10% FBS was added to the cells and placed back in the incubator at 37 °C and 5% CO₂. After overnight incubation, media was aspirated, discarded, and replaced with 20 mL fresh dMEM media with 10% FBS. Cells were placed back in incubator for another overnight incubation period. Forty-eight hours post transfection, media was harvested and replaced a second time with fresh dMEM media with 10% FBS. Harvested media was stored at 4°C. This process was

repeated 72 hours post transfection in a similar manner. If needed, packaged viral vectors can be concentrated.

Once the amount of virus to be added was determined, B-ALL cell lines were plated in 6-well plates and allowed to grow to about 70% confluency. Two concentrations of virus were added to cells to determine the successful transduction efficiency. On the day of transduction, viral stock, 2 μ L 4 mg/mL polybrene and 1 mL IMDM (ATCC) were combined and added to the cells in a 6-well plate. The 6-well plates were centrifuged at 2500 rpm for 100 minutes at 32 °C. Twenty-four hours post transduction, 1 mL of fresh media was added to samples in the 6-well plate to reduce any possibility of cell death. Forty-eight hours post transduction, the transduction protocol was repeated, and the cells allowed to rest for an additional 24 hours. Ninety-six hours post transduction, cells were surface stained with anti-human HLA-A2 (BB7.2)-FITC antibody and sorted for HLA-A2⁺ (FITC⁺) cells using FACS Aria IIIu #1 Cell Sorter (BD). Cells were re-sorted once a month to ensure that cells not successfully transduced would not overcome the culture and give false results in experiments.

2.3 Generation of Protein Lysates and Western Blots

Approximately 2×10^6 cells were lysed in 50 μ L of RIPA lysis buffer 1X with protease inhibitor (Santa Cruz Biotechnology) (ten μ L of protease inhibitor were added to 1 mL of RIPA buffer), and then rotated at 4 °C for 30 minutes. Protein concentration was measured by a Bradford assay. The volume of each protein lysate used was dependent on the protein concentration, but approximately 20 μ g of total protein was aliquoted. Five microliters of loading dye was added to each sample, then vortexed, spun down, and boiled for ten minutes to denature the proteins for SDS-PAGE.

Whole cell lysates were separated by electrophoresis on a 10% SDS gel (BioRad), and transferred to a polyvinylidene difluoride (PVDF) membrane. The membrane was blocked in 5% milk in TBS-TWEEN for 1 hour at room temperature. Primary antibody was added to blocking buffer at the proper dilution and allowed to rotate with the membrane overnight at 4 °C. Membrane was then washed with 0.05% TBS-TWEEN 3x for 8 minutes each. The blot was then incubated with the appropriate secondary antibody in 5% milk blocking buffer at room temperature for 1 hour with rotation. Membranes were then washed with 0.05% TBS-TWEEN 3 times for 8 minutes each wash. Antibodies used included mouse anti-NE, clone NP57 (Santa Cruz Biotechnology), anti-P3, clone MFPR3-2 (ThermoFisher Scientific) and mouse anti-actin, Clone C4 (Millipore). During final wash, an ECL reagent mixture was prepared. The reagent is BioRad Clarity at a 1:1 mixture with 7 mL total for each blot. ECL reagent was added to the blot and incubated at room temperature for 5 minutes. The blot was then imaged using ChemiDoc Touch Imaging System (BioRad).

2.4 RNA Purification and RT-PCR

To purify RNA, the RNeasy Plus Mini Kit (Qiagen) was used per manufacturers instructions. 10×10^7 tumor cells were harvested and 600 μ L of Buffer RLT with beta-mercapotoethanol (B-ME) and vortexed for 30 seconds. Solution was transferred to a gDNA Eliminator spin column and placed into a 2 mL collection tube. Samples are centrifuged for 30 seconds at 8000g and the column is discarded while the flow through is kept. Six hundred microliters of 70% ethanol is added to the flow-through and mixed well with a pipette. Seven hundred microliters of the samples is then added to an RNeasy spin column, placed in a 2 mL collection tube, and centrifuged for 15 seconds at 8000g. The flow-through in this case is discarded and the filter is kept. Five hundred

microliters of Buffer RPE is added to the RNeasy spin column and centrifuged for 15 seconds at 8000g. Five hundred microliters of Buffer RPE is added again to the RNeasy spin column and this time centrifuged for 2 minutes at 8000g. The spin column is then placed into a 1.5 mL eppendorf tube and 30-50 μ L of RNase-free water is directly added to the spin column membrane. The RNA is eluted by a last centrifugation step of 1 minute at 8000g. The concentration of the sample is read on a Synthesizer of cDNA was performed using the Gene Amp RNA kit (PerkinElmer). The following primers were ordered from Sigma-Aldrich: *ELANE* (forward 5'-CACGGAGGGGGAGAGACC-3'; reverse 5'-TATTGTGCCAGATGCTGGAG-3') and *PRTN3* (forward 5'-GACCCCACCATGGCTCAC -3; reverse 5'-ATGGGAAGGACAGACAGGAG-3'). ACTIN (forward 5'-CCAGAGCAAGAGAGCTATCC-3'; reverse 5'-CTGTGGTGGTGAAGCTGTAG-3') served as a loading control. Following denaturation for 5 minutes at 95 °C, samples were amplified for 35 cycles using an iCycler iQ thermal cycler (Bio-Rad Laboratories). Samples were run on a 1.5% agarose gel and bands were imaged using GelDoc2000 (Bio-Rad Laboratories) and analyzed by Quantity One software (Bio-Rad Laboratories).

2.5 NE and P3 uptake in B-ALL cell lines

Analysis of uptake of NE and P3 in B-ALL cell line was carried out by standard flow cytometry methods. Cells were co-cultured in reduced serum medium (0.5% FBS) with 10 μ g/mL soluble NE (Lee), soluble P3 (Athens), irradiated PMN (7500 cGy), or resting PMNs at a ratio of 3:1 (PMN: B-ALL cell). After co-incubation, B-ALL cells were washed in cold phosphate-buffered saline (PBS) (Lonza), and then stained for B-ALL surface markers along with Live/Dead Fixable Aqua (Tonbo). Cells that were co-cultured with healthy PMNs were also cultured with IVIG at 1:10 ratio diluted in PBS.

Because PMNs are very high in Fc receptor expression, there can be a significant amount of non-specific binding. Addition of IVIG to the staining process will inhibit this. After surface staining, cells were washed in PBS, fixed in 1% formaldehyde (ThermoFisher Scientific) in PBS and permeabilized in 5% Perm/Wash Buffer (BD). Uptake of NE and P3 was then determined by staining with Anti-NE-AF647 and Anti-P3-AF488. Samples were analyzed on the LSRFortessa Analyzer, and analyzed via Flowjo software (Treestar Ashland OR).

2.6 PR1 Cross-Presentation

To determine PR1 cross-presentation, B-ALL cell lines were co-cultured with 10 µg/mL of soluble NE, soluble P3, and with irradiated (7500 cGy) PMNs at a ratio of 3:1 (irradiated cell: B-ALL cell) in reduced serum media (0.5% FBS). Cells were then surface stained with B- ALL phenotypic markers (anti-CD19-PE (BioLegend), anti-CD34-AF700 (BioLegend), anti-CD38-Per/Cy7 (BioLegend), anti-CD10-BV421 (BioLegend)) at a 1:50 dilution, Aqua Live Dead (Tonbo) stain at a 1:100 dilution, anti-human 8F4-AF647 (made in house) to identify PR1 cross-presentation at a 1:100 dilution, and finally with anti-human HLA-A2 (BB7.2)-FITC (BioLegend) at a 1:50 dilution, as previously described⁴. Incubation was for 30 minutes on ice. Cells were washed once more in cold PBS, and fixed in 1% formaldehyde. T2 cells pulsed with PR1 and CG1 peptide (Bio-synthesis Inc., Lewisville, TX, USA) were used as a positive and negative control, respectively. T2 cells are commonly used in studying antigen recognition by CTLs through administering exogenous antigen where they are bound and displayed on MHC class I molecules. They are however deficient in a peptide transporter involved in antigen processing (TAP) and therefore do not transport antigen to the endoplasmic reticulum (ER)/Golgi apparatus⁴⁷ to be bound to MHC class I

molecules. Therefore, when pulsed with a peptide of interest, CTL response can be determined in a non-competitive environment. When pulsed with PR1, the peptide will bind to the HLA-A2 molecule on the cell surface and can therefore bind to 8F4 antibody. Samples were collected on a BD LSRFortessa, analyzed on FlowJo software (Tree Star) and graphed with GraphPad Prism.

2.7 PR1-specific CTLs

To expand PR1-specific CTLs, DCs were matured from adherent monocytes and then used as professional APCs. Healthy peripheral blood mononuclear cells (PBMC) isolated from a buffy coat were adhered to a 6 well plate at 37 °C in Macrophage Serum Free Medium. Lymphocytes from the same donor were separated and co-cultured with 40 µg/mL of PR1. For five days, cells were then stimulated with interleukin (IL)-7 (10ng/mL) (rhIL-7, carrier free; BioLegend) and IL-2 (10 ng/mL) (rhIL-2; R&D) Adhered monocytes were matured into monocyte-derived DC through the addition of granulocyte macrophage colony-stimulating factor (GM-CSF) (100 ng/mL)(Sanofi), IL-4 (50 ng/mL) (rhIL-4, carrier free; Tonbo Biosciences) and tumor necrosis factor (TNF)- α (25 ng/mL) (rhTNF- α ; BioLegend). After 5 days, DCs were detached from the 6 well plates, co-cultured with PR1 peptide at 40 µg/mL and combined with expanded lymphocyte population. The co-culture of mature DCs with lymphocytes was stimulated once again with IL-7 (10 ng/mL) and IL-2 (25 ng/mL) for an additional 7 days to induce proliferation. On day 14 of stimulation, cells were harvested and analyzed via flow cytometry by PR1 dextramer staining to determine the percentage of antigen-specific cells that were generated.

2.8 PR1-CTL Cytotoxicity Assay

A standard cytotoxicity assay was used in determining specific lysis, as previously described^{16,17}. HLA-A2 positive cells were co-cultured overnight with soluble NE and P3 (10 µg/mL), washed in RPMI 1640 (HyClone), and resuspended at 1.0×10^5 cells/mL. Cells were then stained with calcein-AM (Invitrogen) at a 1:200 dilution for 15 minutes at 37 °C. Stained cells were then washed three times in RPMI 1640, and resuspended once again at 2.0×10^5 cells/mL. Ten microliters of stained cells were added to a Terasaki plate and co-cultured with PR1-specific CTLs at 5 various ratios (10:1; 5:1; 2.5:1; 1.25:1; 0.625:1 (PR1-CTLs: B-ALL)). Plates were spun at 1500 rpm for 60 seconds and incubated for four hours at 37 °C in 5% CO₂. Wells with target cells alone and medium alone were used as maximum and minimum fluorescence emission, respectively. After incubation period, 5 µL of trypan blue was added to each well and a microplate fluorescence reader then quantified fluorescence. A decrease in the emission of fluorescence was indicative of a reduced specific lysis as the trypan blue quenches the hemoglobin contained in the calcein-AM reagent. With values given, percentage specific lysis was calculated by using the formula:

$$(1 - [\text{fluorescence}_{\text{target + effector}} - \text{fluorescence}_{\text{media}}] / [\text{fluorescence}_{\text{target alone}} - \text{fluorescence}_{\text{media}}]) \times 100.$$

T2 cells pulsed with PR1 and CG1 peptide was used as positive and negative controls, respectively.

2.9 Induction of NET formation and identification via flow cytometry

PMNs from a healthy donor were derived by an already established density gradient centrifugation protocol using Histopaque 1077 and 1019. 1×10^6 PMNs were

placed in a FACS tube, treated with Ionomycin (4 μ M) (Sigma) or Phorbol-1-myristate-13-acetate (PMA)(100 nM) (Sigma Aldrich) and incubated for four hours at 37 °C with 5% CO₂ in air. Cells were then fixed in 2% formaldehyde, blocked for 30 minutes in 2% bovine serum albumin in PBS at 37°C, and stained with primary rabbit anti-human histone H3 antibody (citrulline 2,8,17) (Abcam) at a 1:300 dilution, AF647 goat anti-rabbit IgG (H+L) secondary antibody (Invitrogen) at a 1:300 dilution and FITC-conjugated anti-MPO antibody (BioLegend) at a 1:50 dilution. Each incubation period was 30 minutes. After every incubation, the samples were washed in PBS with 2% BSA and then centrifuged at 16,400 rpm at 4 °C for 20 minutes. Lastly, samples were stained with Hoechst 33342, trihydrochloride trihydrate (Thermo Scientific) in 2% BSA in PBS at a 1:5000 dilution. Analysis was conducted by flow cytometry. Gating strategy included first on DAPI positive cells, then on cells positive for H3 citrullination, an early marker of NETosis, and lastly on MPO positive cells. Cells marked as triple positive were considered PMNs undergoing NETosis.

2.10 Identification of NETs via confocal microscopy

To perform confocal microscopy, coverslips were first pretreated with 0.001% poly-L-lysine. Healthy donor neutrophils were treated with PMA (100 nM) or Ionomycin (4 μ M) and then incubated at 37 °C for four hours. NETs were then fixed in 4% formaldehyde and incubated for 30 minutes at room temperature. Coverslips were washed in PBS, blocked with 5% donkey serum and 0.5% Triton X in PBS, and incubated at 4 °C overnight. Coverslips were then stained in anti-MPO-FITC or anti-P3-AF488, anti-NE-AF647, and Hoechst. Lastly, coverslips were placed on a slide with prolong gold without DAPI, and sealed with nail polish. Confocal images to show NET formation were taken using a Leica Microsystems SP2 SE confocal microscope (Leica)

with x 10/25 air, x63/1.4 oil objectives and analyzed using Leica LCS software.

2.11 Determine whether NETs are a source of NE and P3 uptake

NET formation was induced in a manner similar to what has been previously described ⁴⁸. After a 4-hour incubation at 37 °C, NETs were co-cultured with B-cell ALL cell lines overnight. At this time point, cells were then stained with fluorescently conjugated B-cell ALL phenotypic markers along with life/dead aqua, fixed in 1% formaldehyde and permeabilized in 5% Perm/Wash Buffer (BD) in deionized water. Once permeabilized, cells were stained with anti-NE-AF647 and anti-P3-AF488 to determine uptake by flow cytometry. We hypothesized that uptake would occur due to the presence of NE and P3 localized in the NETs once released into the tumor microenvironment. The first four conditions listed below are necessary in determining whether NET-associated NE and P3 are taken up. Intracellular staining in B-ALL cell lines alone and B-ALL cell lines co-cultured with PMNs were used as a negative and positive control, respectively. The latter was used as a positive control as we have already shown PMN-associated NE and P3 uptake occurs in B-ALL cell lines (Figure 6-7).

1. B-ALL cell line alone (negative control)
2. Resting PMN + B-ALL cell line (positive control)
3. (Ionomycin + PMN (NETs)) + B-ALL cell line
4. (Ionomycin + DNase + PMN) + B-ALL cell line

Publications have previously shown that the integrity of the DNA backbone in NETs is necessary to maintain proteolytic activity and conformation of antimicrobial proteases to promote uptake and mDC activation ⁴⁵. Therefore, NETs were treated with DNase (100 U/mL) (Sigma Aldrich) after inducing NETosis to disrupt the structure of

the protease/DNA interaction, co-cultured with B-ALL cell lines overnight and stained for intracellular uptake of NE and P3. It was also important to differentiate between NET-associated NE and P3 uptake and the effects of Ionomycin and DNase treatment on uptake. Therefore, conditions listed below were done to prove that any uptake seen in ALL co-cultured with NETs was indeed NET-associated NE and P3 uptake.

5. DNase + PMN + ALL cell line
6. Irradiated PMN + ALL cell line
7. DNase + Irradiated PMN + ALL cell line
8. Soluble NE/Soluble P3 + ALL cell line
9. Ionomycin + Soluble NE/Soluble P3 + ALL cell line
10. DNase + Soluble NE/Soluble P3 + ALL cell line

In comparing the efficiency of uptake between possible sources of NE and P3 in the microenvironment, it was also important to determine the spontaneous ability of resting and irradiated (7500 cGy) PMNs to undergo NETosis. To achieve this, cells at each condition were incubated sequentially with primary anti-histone H3 antibody at 1:300 dilution, AF647 goat anti-rabbit IgG (H+L) secondary antibody at 1:300 dilution, and anti-MPO-FITC antibody at a 1:50 dilution. Each incubation was followed by a wash with 2% BSA in PBS and centrifuged at 1500 rpm at 4°C for five minutes. Samples were then resuspended in Hoechst 333342, trihydrochloride, trihydrate at 1:5000 dilution and analyzed via flow cytometry.

Chapter Three: Results

3.1 B-ALL cell lines cross-present PR1 rendering them susceptible to killing by PR1-targeting immunotherapy

3.1.1 B-ALL cell lines Lack Intracellular Expression of NE and P3

Because B cell ALL is a non-myeloid malignancy, it is expected to lack endogenous expression of NE and P3. Therefore, any PR1/HLA-A2 surface expression was attributed to NE and P3 uptake and PR1 cross-presentation. To confirm lack of endogenous expression of NE and P3, mRNA expression levels were first confirmed on public data provided by CCLE (Cancer Cell Line Encyclopedia) and then ALL cell lines were analyzed via RT-PCR, western blot, and flow cytometry. Lack of endogenous NE and P3 expression was confirmed in the panel of B-ALL cell lines, in agreement with publically available data from the Cancer Cell Line Encyclopedia (CCLE) (Figure 1A/Figure 2A). Based on RT-PCR conducted, when compared to positive control (AML cell line U937) and negative control (multiple myeloma (MM) cell line U266), all four B-ALL cell lines show lack of endogenous (Figure 1B) NE and (Figure 2B) P3 mRNA expression levels. Next, protein expression levels were analyzed. Positive and negative controls for protein expression included AML cell like U937 along with soluble NE/P3 and breast cancer cell line MDA-MB-231, respectively. In comparison with positive and negative controls, there also is a lack of endogenous NE (Figure 1C) and P3 (Figure 2C) protein expression in all four cell lines. Lastly, intracellular expression was analyzed via flow cytometry. Cells were stained with live/dead aqua, fixed in 1% formaldehyde, permeabilized in 5% perm solution and stained for intracellular expression with anti-NE-Alexa Fluor (AF) 647 and anti-P3-AF488. Positive and

negative controls for intracellular expression were AML cell line U937 and breast cancer cell line T47D, respectively. In comparison, a lack of endogenous intracellular expression of NE (Figure 1D) and P3 (Figure 2D) was evident as well. Based on all four methods, it was confirmed that all four lymphoblastic leukemia cell lines lack endogenous expression of NE and P3. Therefore, any intracellular expression seen in the presence of the aforementioned proteases was attributed to NE and P3 uptake.

3.1.2 B-ALL cell lines take up soluble and PMN-associated NE and P3

Because we have previously shown that NE and P3 uptake occurred in APCs, including B cells⁷, and the high expression of NE and P3 in the bone marrow, we hypothesized the ALL cells take up NE and P3. B-ALL cell lines SB, Nalm6, RS4 and SupB15 were co-cultured with 10 µg soluble NE and P3 at 10 minutes (Figure 3A-B) and overnight time points (Figure 3C-D) and analyzed for intracellular uptake using flow cytometry. Data indicated that uptake occurred in all four cell lines at both time points, although at varying extents. Data shown displays the mean fluorescence intensity (MFI) of pulsed versus non-pulsed ALL cells (Figure 3). The MFI following NE uptake at ten minutes ranged from 210 to 587 (Figure 3A). Similar results were seen in P3 with a range of uptake varying from MFI 464 to 1854 (Figure 3B). Overnight uptake was similarly calculated for both NE and P3. The extent of NE uptake ranged from MFI 340 to 6166 (Figure 3C). A similar pattern was seen for soluble P3 at the overnight time point with MFI ranging from 1629 to 7704 (Figure 3D). We further identified a time-dependent increase in both NE and P3 uptake in SupB15, Nalm6, SB, and RS4 B-ALL cell lines between the 10-minute and overnight time points (Figure 3).

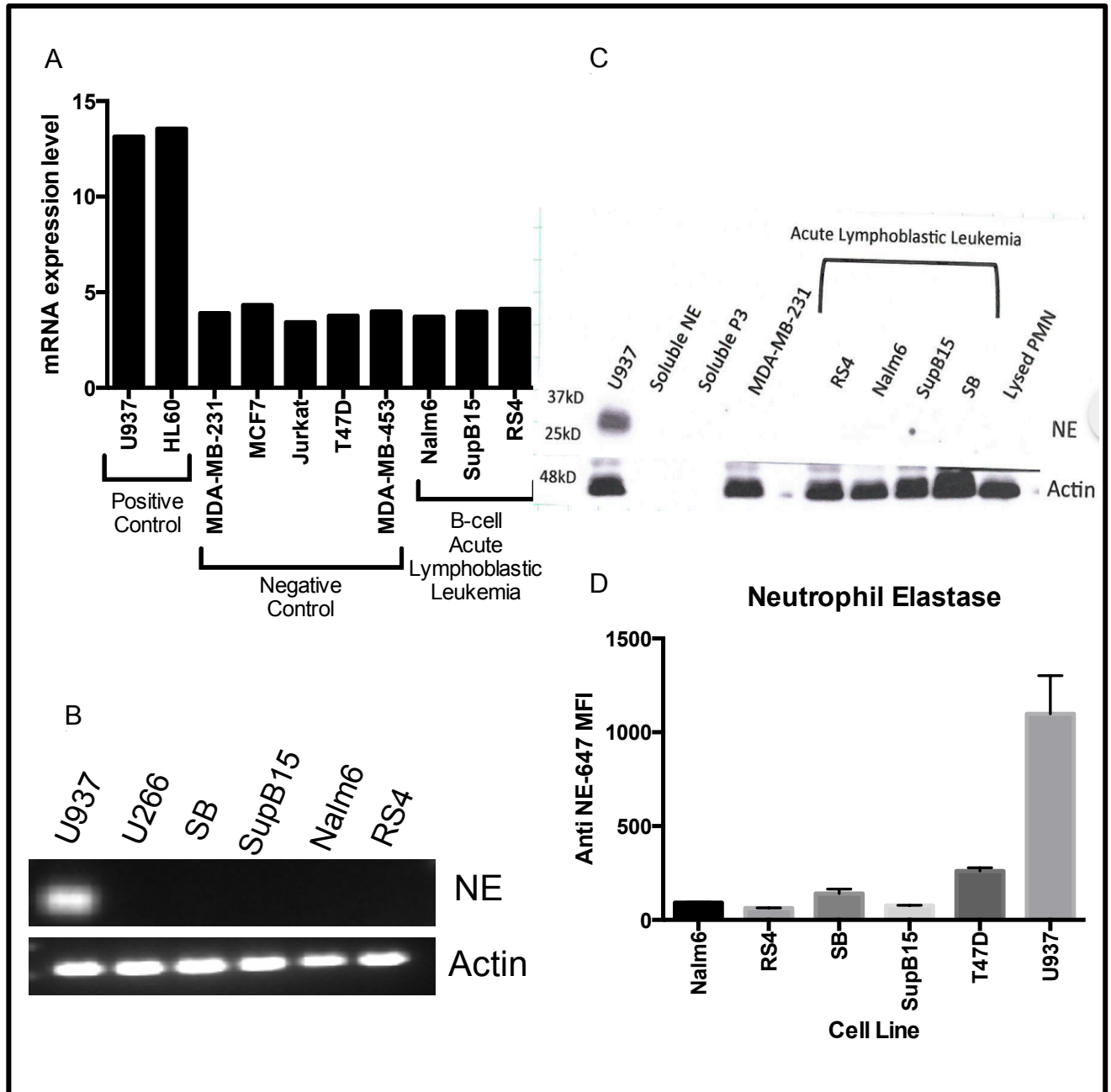


Figure 1: B-ALL cell lines lack endogenous expression of NE. U937 and HL70 were used as positive controls. 231; MCF7, Jurkat, T47D, U266, and 453 cells were used as negative controls. (A) mRNA expression levels were first determined using the Cancer Cell Line Encyclopedia (CCLE). (B) mRNA was extracted from B-ALL cell lines. RT-PCR was performed using NE primers and shows a lack of mRNA expression levels. (C) Western blots demonstrate a lack of NE protein expression. AML cell line U937 was used as a positive control for protein expression and actin was used as a loading control. (D) Flow cytometry shows absence of intracellular NE expression compared to U937, positive control, and T47D, the negative control.

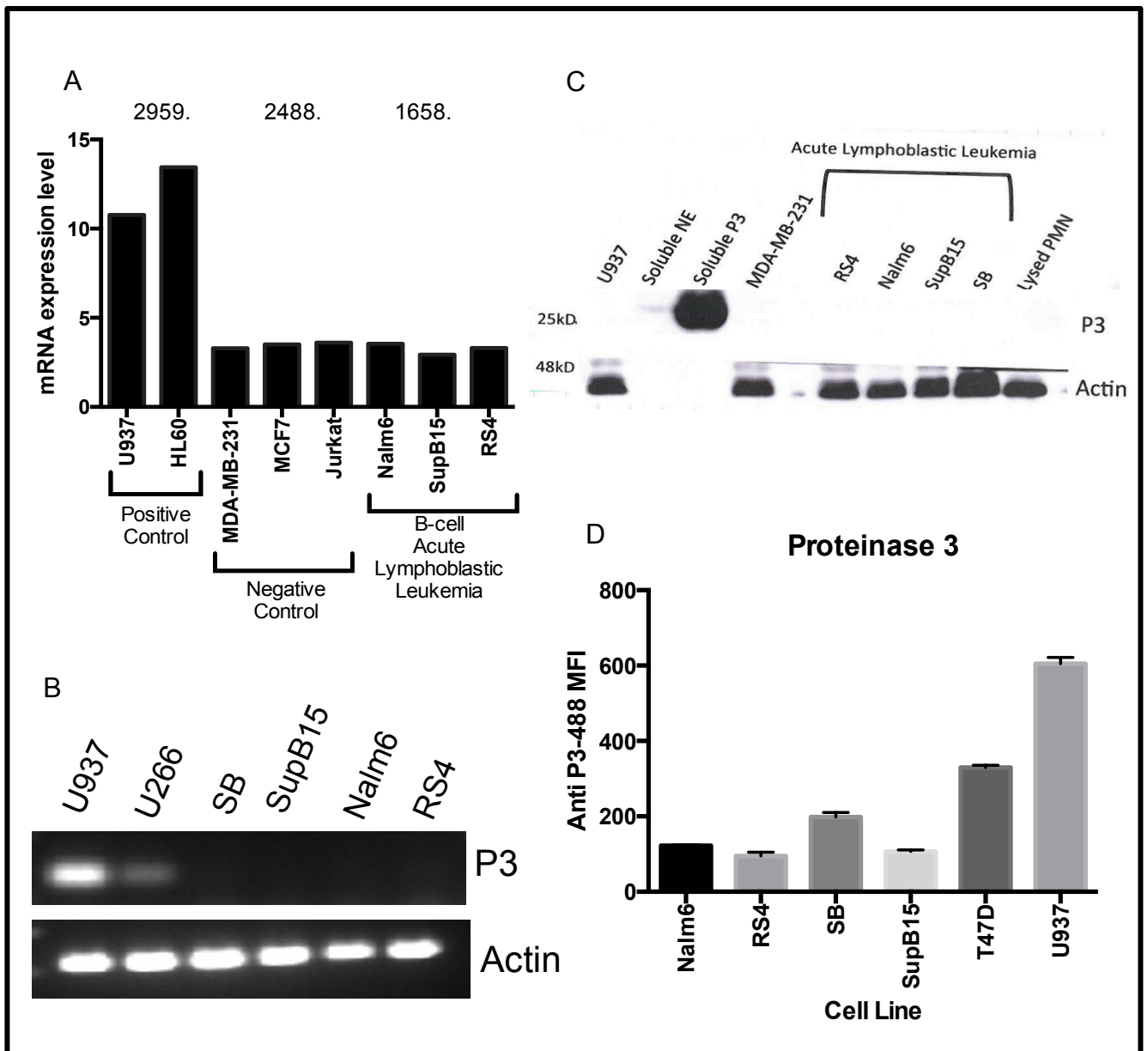


Figure 2: B-ALL cell lines lack endogenous expression of P3. U937 and HL70 were used as positive controls. 231; MCF7, Jurkat, T47D, U266, and 453 cells were used as negative controls. (A) mRNA expression levels were first determined from publically available from the Cancer Cell Line Encyclopedia (CCLE). (B) mRNA was extracted from B-ALL cell lines. RT-PCR was performed using P3 primers and shows a lack of mRNA expression levels. (C) Western blot demonstrates a lack of NE protein expression. Purified P3 (10 ug) was used as a positive control. Actin was used as a loading control. (D) Flow cytometry shows absence of intracellular NE expression compared to U937 and T47D, positive and negative controls, respectively.

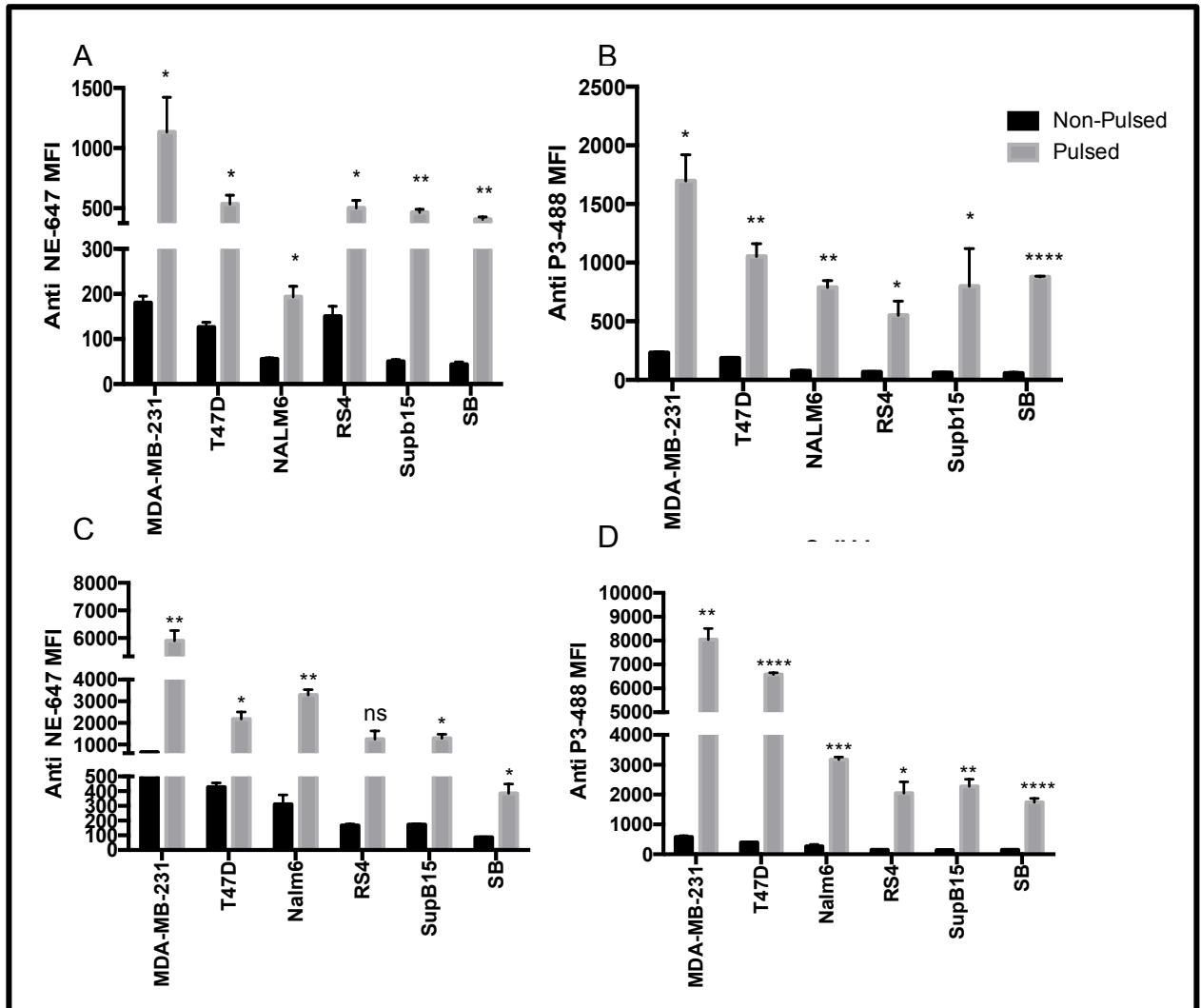


Figure 3: B-ALL cell lines take up soluble NE and P3. (A) Nalm6, RS4, SupB15 and SB cell lines were incubated with soluble NE (10 $\mu\text{g/mL}$) for 10 minutes (A) and 24 hours (C). Similarly all four cell lines were incubated with soluble P3 (10 $\mu\text{g/mL}$) for 10 minutes (B) and 24 hours (D). Samples were then intracellularly stained with anti-NE-AF647 or anti-P3-AF488 and analyzed by flow cytometry for intracellular uptake. Data are means \pm SEM and represent three independent experiments. MFI is plotted on the y-axis.

To confirm that the positive fluorescence via flow cytometry reflected intracellular NE and P3 that resulted from uptake, we co-cultured all four B-ALL cell lines with soluble NE and P3 and acquired real-time images using the ImageStream X Mark II. Cells were co-cultured with soluble NE and P3 (10 µg/mL) overnight, fixed in 1% formaldehyde, permeabilized with 5% perm solution and stained with anti-NE-AF647, anti-P3-AF488, and Hoechst-33342. Data indicated that all B-ALL cell lines take up NE and P3 when co-cultured with soluble proteases indicated by intracellular positive fluorescence (Figure 4).

In further studying the kinetics of NE and P3 uptake, we wanted to determine the degree of uptake over time. SB, Nalm6, RS4 and SupB15 cell lines were co-cultured with soluble NE and P3 (10 µg/mL) for 1 hour, 2 hours, 4 hours, 6 hours, and 24 hours. After each incubation period, cells were stained with Live/Dead Aqua, fixed in 1% formaldehyde, permeabilized in 5% perm solution, and intracellular stained with anti-NE-AF647 and anti-P3-AF488. Data confirmed earlier results describing the variance in the degree of uptake between each cell line (Figure 5). Further, after 1 hour of co-culture, uptake of both NE and P3 plateaus over time, suggesting a receptor-mediated process for both NE and P3 uptake (Figure 5).

Different cellular pathways are involved in the uptake and processing of soluble versus cell-associated proteins. This can then determine whether or not they are cross-presented. We therefore evaluated whether there was a difference between the uptake of soluble and cell-associated NE and P3 in B-ALL cell lines. Each cell line was co-cultured at 3 hours and 24 hours with soluble NE and P3 (10 µg/mL), irradiated PMNs (7500 cGy) and resting PMNs at a ratio of 3:1 (PMN:B-ALL). PMN and PBMCs

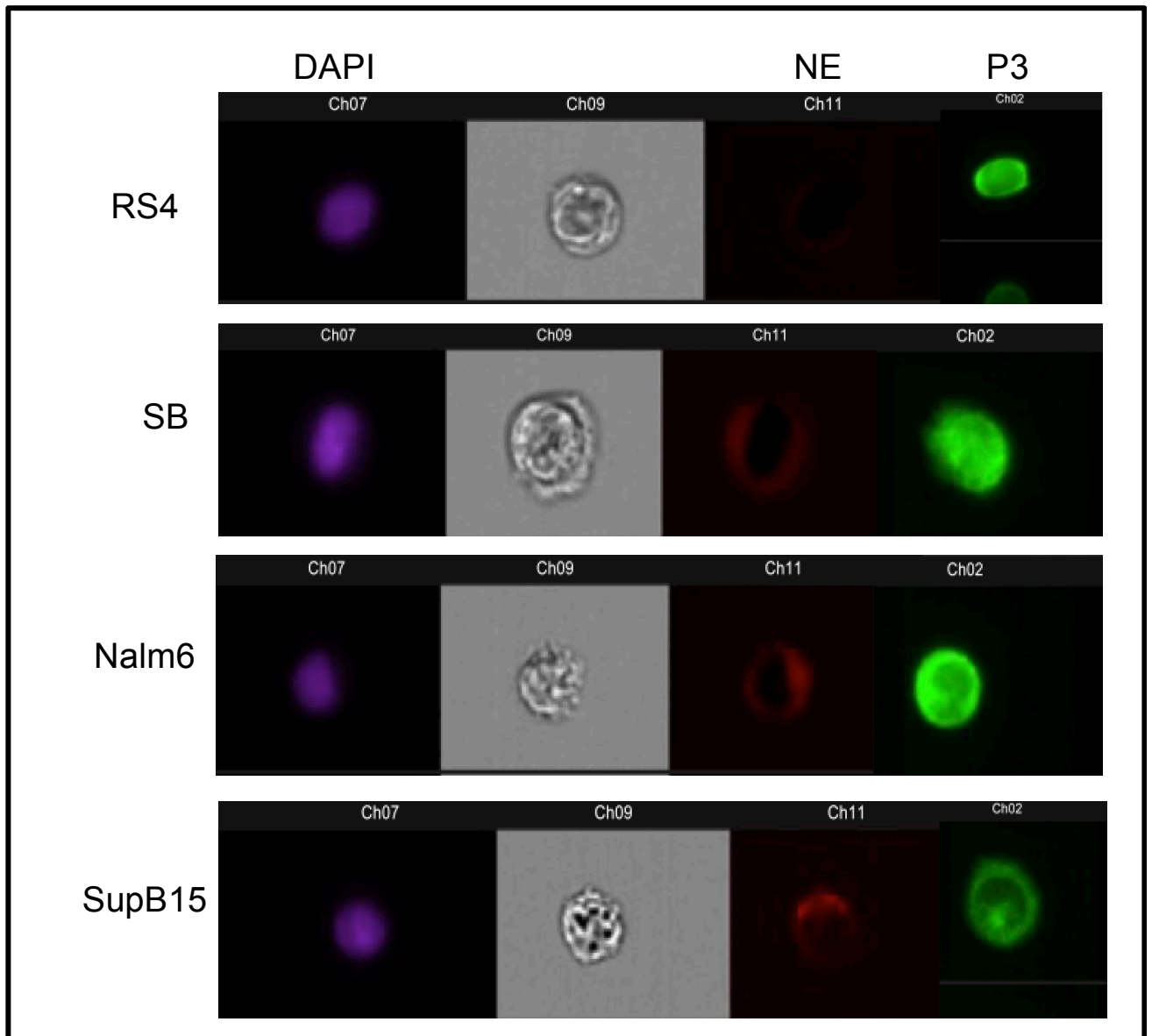


Figure 4: Intracellular uptake of NE and P3 occurs in RS4, SB, Nalm6 and SupB15 B-ALL cell lines. To confirm that NE and P3 expression indicated by flow cytometry was indicative of intracellular uptake, B-ALL cell lines were co-cultured with soluble NE and P3 (10 $\mu\text{g}/\text{mL}$) overnight. After co-culture, cells were fixed in 1% formaldehyde, permeabilized in 5% perm solution, and intracellularly stained with anti-NE-AF647, anti-P3-AF488, and DAPI. Samples were analyzed on the ImageStreamX Mark II.. Channel 7 indicates DAPI expression; channel 9 of side scatter, channel 11 indicative of NE expression and channel 2 on P3 expression.

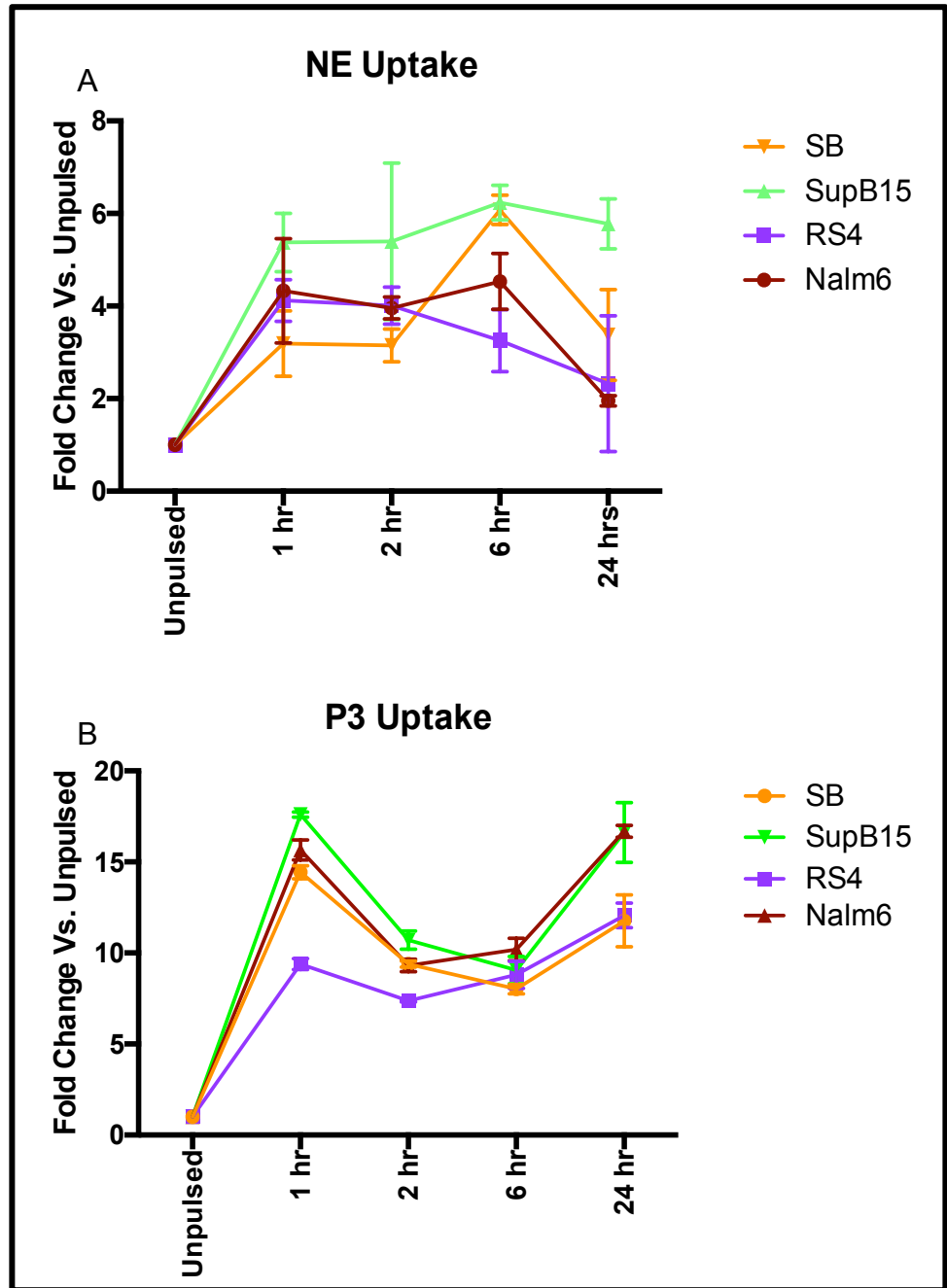


Figure 5: Uptake of soluble NE and P3 plateaus over time in B-ALL cell lines. SB, Supb15, RS4 and Nalm6 B-ALL cell lines were co-cultured with soluble NE and P3 (10 μ g/mL) at increasing time points, and analyzed for uptake of (A) NE and (B) P3. Fold increase of the MFI of NE or P3 versus unpulsed cells is shown on the y-axis. Data indicated that after 1 hour of co-culture, both NE and P3 uptake plateaus indicative of receptor-mediated uptake.

intracellularly stained for NE and P3 were used as positive and negative staining controls, respectively. Data indicated that all four B-ALL cell lines took up both soluble and PMN-associated NE (Figure 6) and P3 (Figure 7). In fact, uptake from the PMN source was more efficient compared with uptake from soluble NE and P3 (Figure 6-7). This may be due to the association of NE and P3 with other neutrophilic proteins that could play a role in assisting in uptake of NE and P3. Similarly to soluble NE and P3, the degree of uptake of PMN-associated proteases varied among cell lines. SupB15 and RS4 took up PMN-associated NE and P3 (Figure 6/7C-D) at the greatest extent, and although Nalm6 and SB cell lines also took up P3, it was at a significantly lesser extent than that of soluble (Figure 6/7A-C). Tables 2 and 3 display the fold increase in MFI versus unpulsed cells of PMN-associated and soluble uptake. This data is representative of data showing uptake of PMN-associated versus soluble (Figure 6-7).

Together our results showed that B-ALL cell lines lack endogenous NE and P3 but can internalize NE and P3 from exogenous sources.

3.1.3 P3 is taken up at a greater extent than NE in B-ALL cell lines

To further characterize NE and P3 uptake, we next sought to compare the efficiency of NE versus P3 uptake. We co-cultured B-ALL cell lines, SB, Nalm6, SupB15 and RS4, with soluble NE and P3 (10 µg/mL) and resting healthy PMNs at a ratio of 3:1 (PMN: B-ALL) overnight, and compared the extent of intracellular uptake. Our data showed significantly greater uptake of PMN-associated and soluble P3 compared with PMN-associated and soluble NE in the SB, Nalm6 and RS4 cell lines (Figure 8A-C). This result was consistent with prior data from our lab showing that P3 uptake was greater than NE uptake⁶. However, in SupB15 cell line, there was no significant difference between the uptake of cell-associated and soluble NE and P3

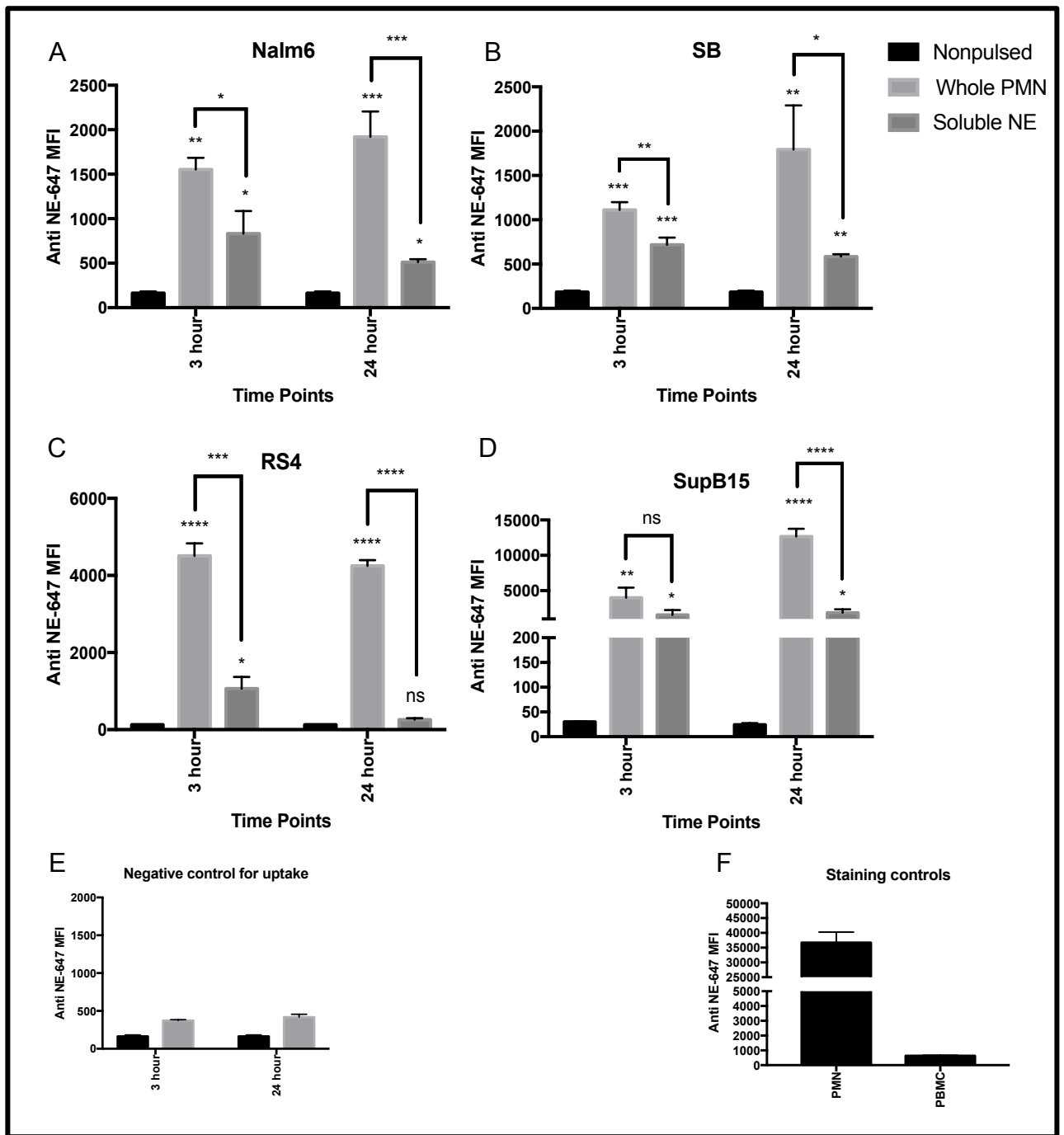


Figure 6: PMN-associated NE is taken up in B-ALL cell lines. Nalm6 (A), SB (B), RS4(C) and SupB15(D) cell lines were co-cultured with resting PMNs at a ratio of 3:1 (PMN: B-ALL) and soluble NE (10 μ g/mL) for 3 hours and 24 hours. Samples were then surface stained for common B-ALL cell markers (CD19, CD34, CD38, CD10) as previously mentioned, fixed in 1% formaldehyde, permeabilized in 5% perm solution, intracellularly stained with anti-NE-AF647 Ab, and analyzed via flow cytometry. (E) B-ALL cell lines were pulsed with PBMCs as a negative control for uptake. (F) PMNs and PBMCs were stained for intracellular NE and P3 as a positive and negative staining control, respectively. Unpulsed cells (black bar) demonstrate baseline staining for NE and P3, as they do not endogenously express either protein (Figure 1/2). Results are representative of two independent experiments. Data indicated that PMN-associated NE is taken up in all B-ALL cell lines at varying extents. Uptake of PMN-associated is also at a greater extent than soluble NE.

Table 2: Uptake of PMN-associated versus soluble NE in B-ALL cell lines

Cell Line	Time Points	PMN Source (Fold Change vs. Unpulsed)	Soluble NE (Fold Change vs. Unpulsed)
SupB15	3 hour	133	51
	24 hour	420	62
RS4	3 hour	35	8
	24 hour	33	2
Nalm6	3 hour	10	5
	24 hour	12	3
SB	3 hour	14	4
	24 hour	11	3

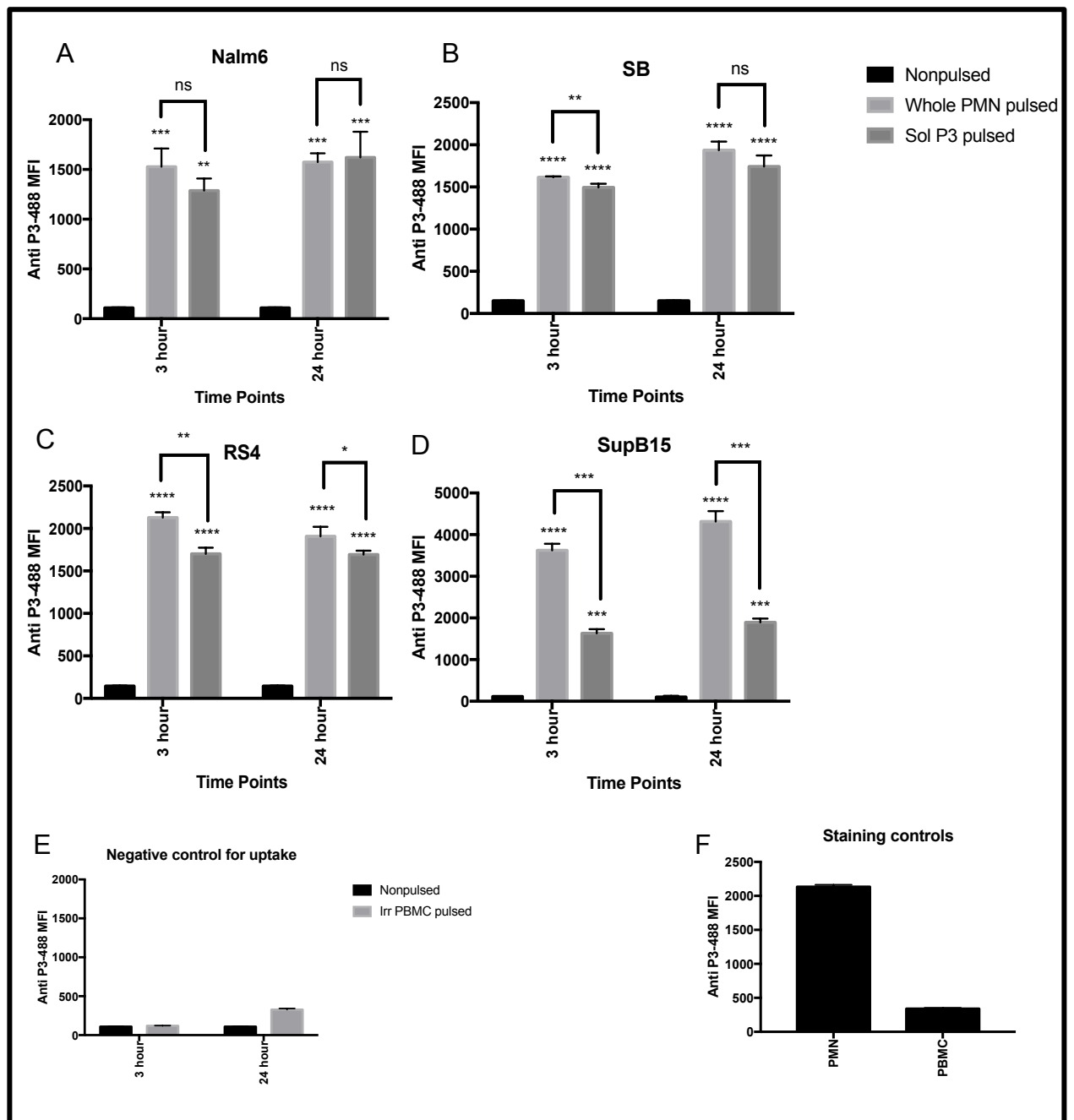


Figure 7: PMN-associated P3 is taken up in B-ALL cell lines. Nalm6 (A), SB (B), RS4 (C) and SupB15 (D) cell lines were co-cultured with PMNs at a ratio of 3:1 (PMN: B-ALL) and soluble NE for 3 hours and 24 hours. Samples were then surface stained for common B-ALL cell markers (CD19, CD34, CD38, CD10), fixed in 1% formaldehyde, permeabilized in 5% perm solution, intracellularly stained with anti-NE-AF647 Ab, and analyzed via flow cytometry. (E) B-ALL cell lines were pulsed with PBMCs as a negative control for uptake. (F) PMNs and PBMCs were stained for intracellular NE and P3 as a positive and negative staining control, respectively. Unpulsed cells (black bar) demonstrate baseline staining for NE and P3, as they do not endogenously express either protein. Results are representative of two independent experiments.

Table 3: Uptake of PMN versus soluble P3 in B-ALL cell lines

Cell Line	Time Points	PMN Source (Fold Change vs. Nonpulsed)	Soluble P3 (Fold Change vs. Nonpulsed)
SupB15	3 hour	33	15
	24 hour	39	17
RS4	3 hour	16	12
	24 hour	16	12
Nalm6	3 hour	14	12
	24 hour	16	15
SB	3 hour	14	10
	24 hour	14	12

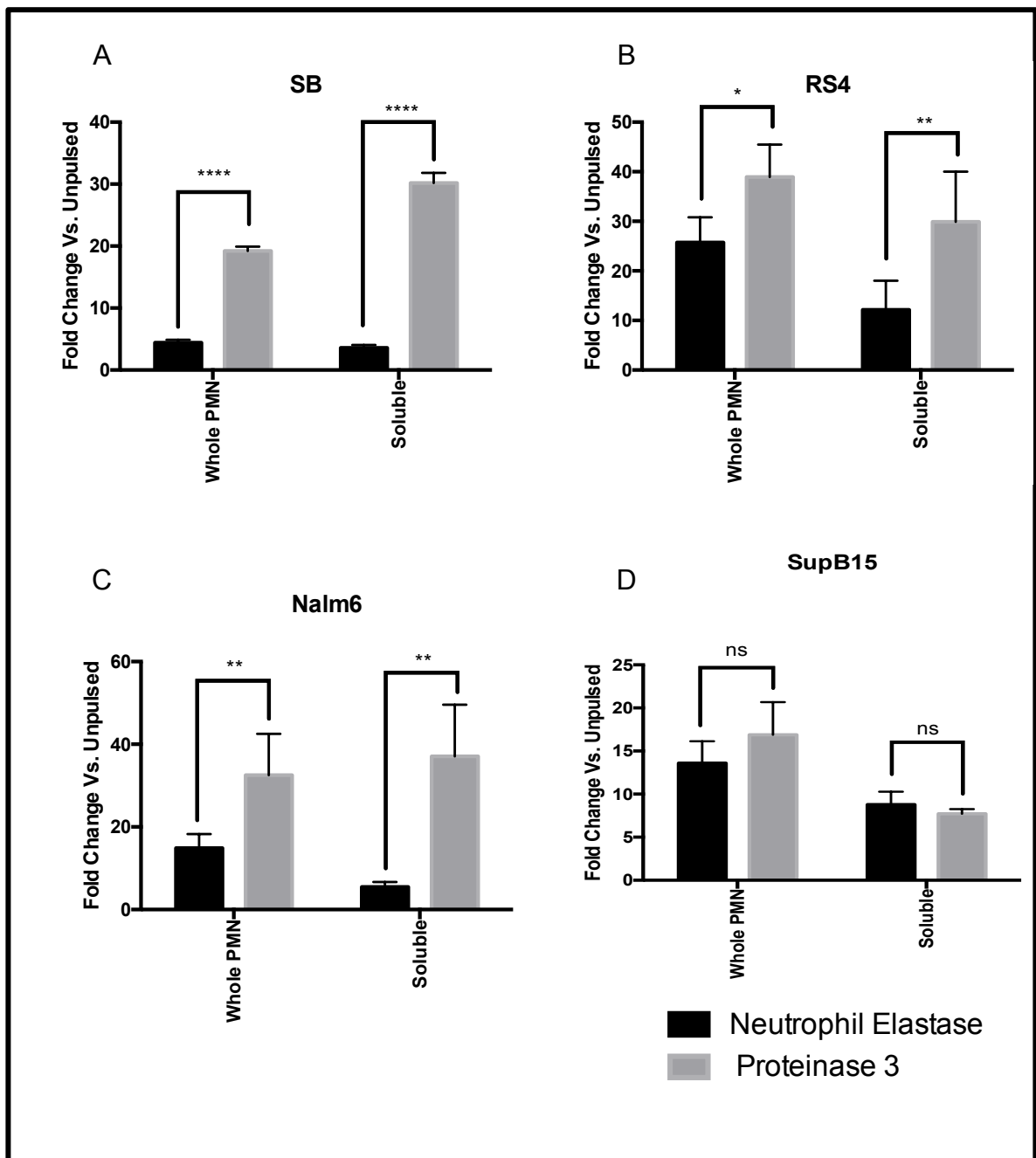


Figure 8: Soluble and PMN-associated P3 is taken up at a greater extent than soluble and PMN-associated NE in Nalm6, RS4 and SB cell lines. B-ALL cell lines were co-cultured with PMN at a ratio of 3:1 (PMN: B-ALL) and soluble NE and P3 overnight. After incubation period, cells were surface stained for B-ALL markers, as previously described, fixed in 1% formaldehyde, permeabilized in 5% perm solution and intracellularly stained with anti-P3-AF488 and anti-NE-AF647. Data indicated that PMN-associated and soluble P3 is taken up at a greater extent than NE in RS4, Nalm6 and SB cell lines. In SupB15 cell line, there was no significant difference in uptake between PMN-associated and soluble NE and P3. Data are means \pm SEM and represent three independent experiments.

(Figure 8D). Data further confirmed the variance in the degree of uptake of both NE and P3 among all four cell lines.

3.1.4 Endogenous HLA-A2 surface expression in B-ALL cell lines

Due to the fact that PR1 is an HLA-A2 restricted peptide, endogenous surface expression of HLA-A2 in SB, Nalm6, SupB15 and RS4 B-ALL cell lines was determined. Two of the four cell lines, SB and Nalm6, were positive for endogenous HLA-A2 surface expression (Fig. 9A-B) compared to that of both nonstained and isotype control staining. Because SupB15 and RS4 cell lines did not endogenously express surface HLA-A2 (Figure 9C-D), they were transduced with a HLA-A2 lentivirus as previously described⁴⁶ in order to further investigate the phenomenon of PR1 cross-presentation. The SupB15 cell line was successfully transduced, as indicated by the increase in MFI compared to nonstained, isotype control, and non-transduced group (Figure 9C). The SB cell line had the highest surface HLA-A2 expression indicated by the highest MFI (MFI = 16,368) compared to that of SupB15 (MFI = 4024) and Nalm6 (MFI = 2368) (Figure 9A-C). These three cell lines were used in all cross-presentation experiments in the subsequent studies.

3.1.5 NE and P3 are cross-presented by B-ALL cell lines

Data up to this point indicated that all four cell lines took up both soluble and PMN-associated NE and P3. Because PR1 is derived from NE and P3, we investigated whether HLA-A2+ B-ALL cell lines cross-present PR1. HLA-A2-positive cell lines, SB, Nalm6 and SupB15, were co-cultured with 10 µg/mL soluble NE/P3 and irradiated PMNs (7500 cGy) for 24 hours to determine whether protease uptake resulted in PR1 cross-

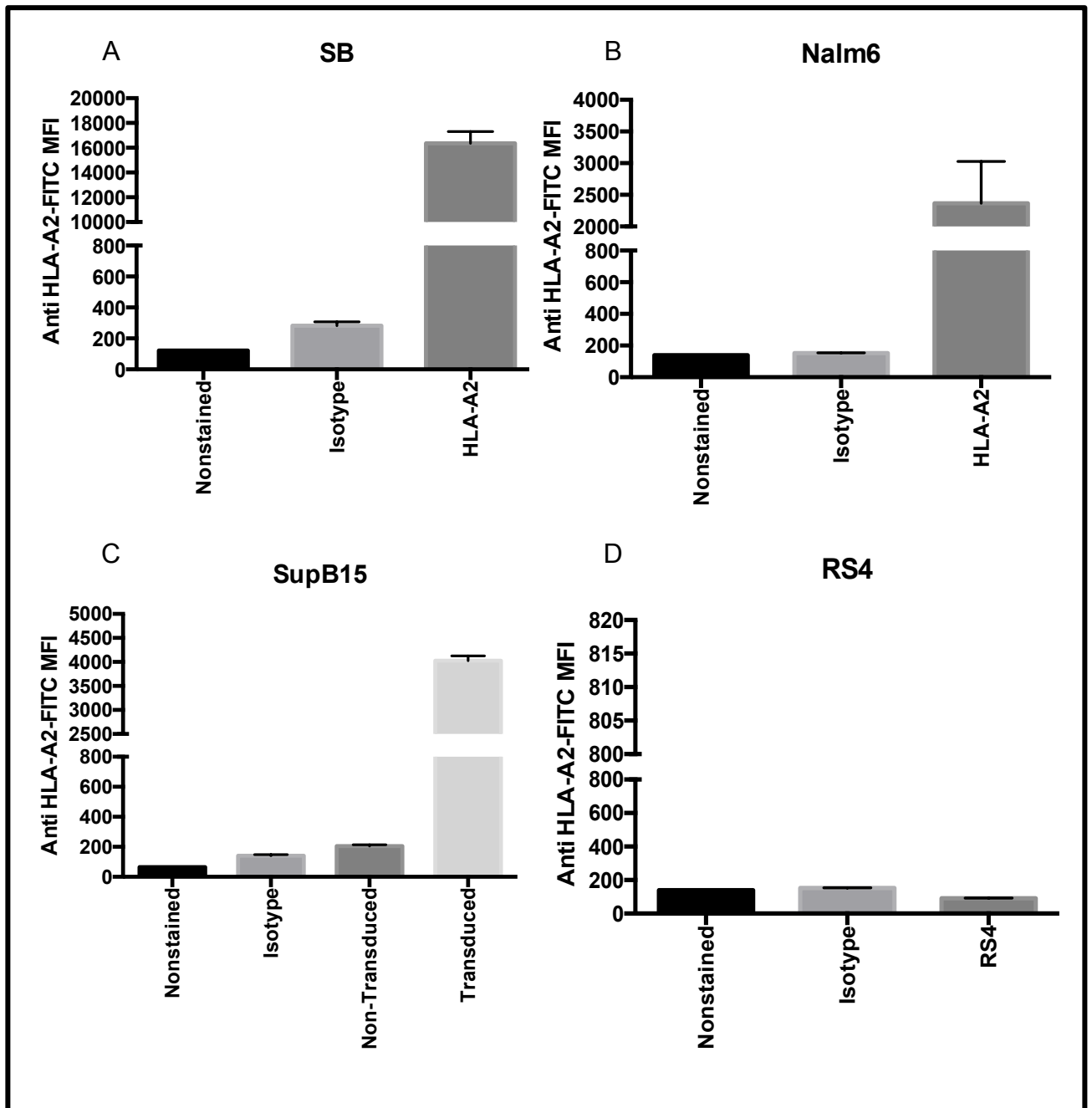


Figure 9: Nalm6 and SB B-ALL cell lines are endogenously HLA-A2 positive. B-ALL cell lines were stained for surface HLA-A2 expression with anti-HLA-A2 (BB7.2)-FITC and analyzed by flow cytometry. MFI was compared to that of isotype control staining and unstained samples. Data indicated that cell lines Nalm6 and SB cell lines were positive for endogenous HLA-A2 surface expression and SupB15 and RS4 negative. After transduction with a lentivirus, SupB15 cell line was positive for surface HLA-A2 expression compared to isotype control, unstained and non-transduced group.

presentation. Cells were analyzed for PR1/HLA-A2 surface expression using the mouse anti-PR1/HLA-A2 antibody 8F4, as previously described^{6,43}. Data showed that the B-ALL cell line, SB, cross-presents PR1 from soluble NE, soluble P3 and PMN-associated proteases (Figure 10A) compared to nonpulsed cells. Cell lines Nalm6 and SupB15 did not cross-present PR1 as indicated by a lack of significant uptake following co-culture with NE and P3 (Figure 10B-C).

3.1.6 PR1 cross-presentation renders B-ALL cell line susceptible to PR1-CTLs

Because PR1 has been effectively targeted in myeloid leukemia using PR1-targeting immunotherapies including PR1 vaccine²⁵, PR1-CTLs² and anti-PR1/HLA-A2 Ab, 8F4^{4,5}, we then investigated whether PR1 cross-presentation by B-ALL, more specifically the SB cell line, rendered it susceptible to killing by PR1-CTLs. Based on previous data showing that the HLA-A2 positive cell line, SB, cross-presents PR1 (Figure 10A), SB cell line was co-cultured with 10 µg/mL soluble NE and P3 for 24 hours and incubated with healthy PR1-CTLs for 4 hours following a protocol for a standard calcein-AM cytotoxicity assay^{15,49}. T2 cells were pulsed with PR1 and CG1 peptide as a positive and negative control, respectively. Data indicated that when co-cultured with PR1-CTLs, there was a dose-dependent killing of SB cells following PR1 cross-presentation compared to nonpulsed cells (Figure 10E). The percent specific lysis when co-cultured with soluble NE and P3 reached a maximum of 30% at higher doses and killing began at a very early ratio of 0.625:1 (Effector: Target) (Figure 10E). T2 cells pulsed with PR1 also had dose-dependent killing by PR1-CTLs, whereas T2 cells pulsed with CG1 and nonpulsed did not get killed, as expected (Figure 10D).

Overall, data indicated that B-ALL cell lines are capable of soluble and PMN-associated NE and P3 uptake, and PR1 cross-presentation rendering B-ALL susceptible to killing by PR1-CTLs.

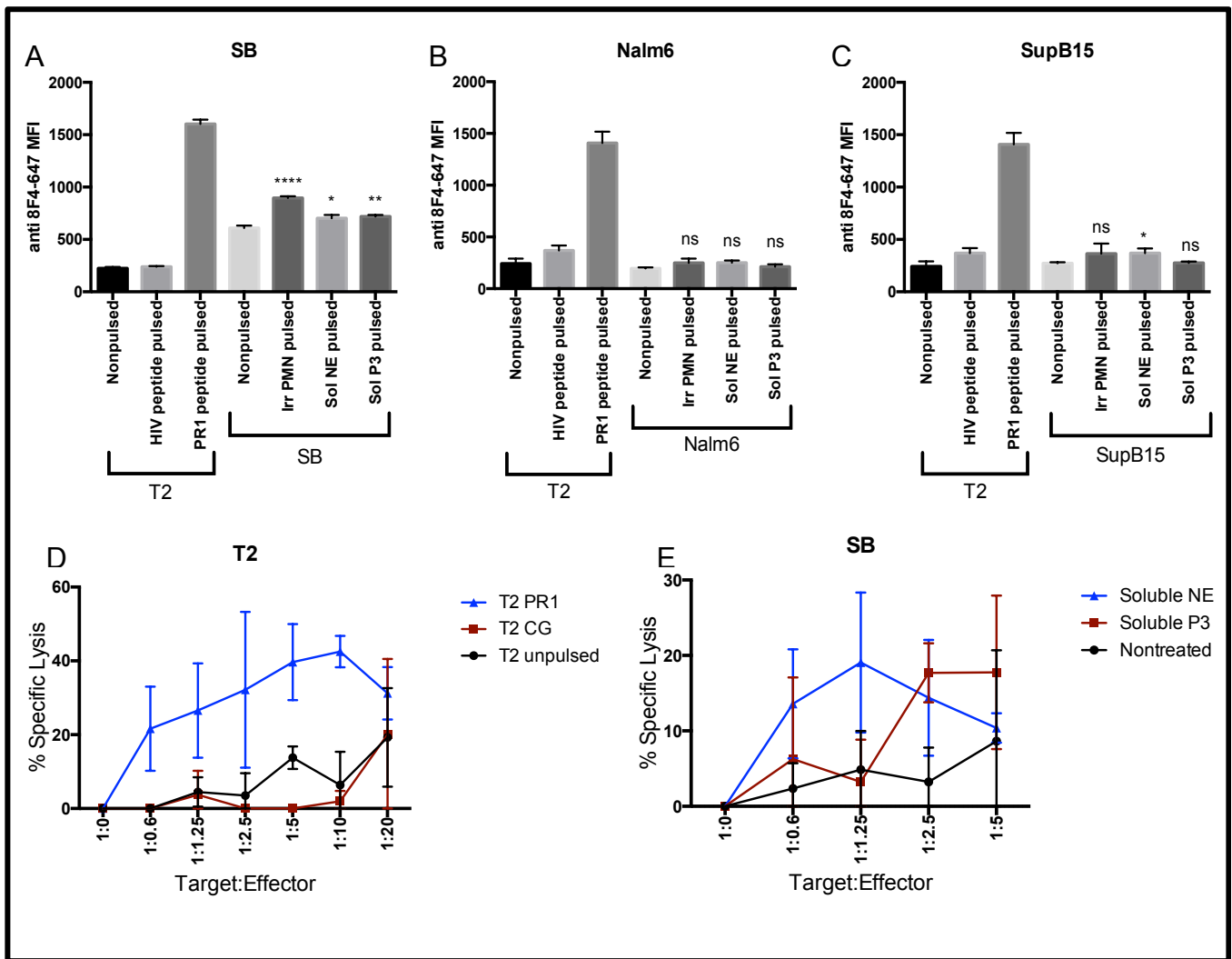


Figure 10: Cross-presentation of soluble NE and P3 increases B-ALL susceptibility to killing by PR1-CTLs. HLA-A2+ B-ALL cell lines (A) SB, (B) Nalm6 and (C) SupB15 were co-cultured with soluble NE and P3 (10 μ g/mL), and irradiated PMNs (7500 cGy) overnight. Cells were analyzed for surface expression of PR1/HLA-A2 with mouse anti-PR1/HLA-A2 Ab, 8F4. Data indicated that of 3 HLA-A2+ cell lines, only SB cell line cross-presents PR1. MFI of PR1/HLA-A2 is shown on the y-axis. 2-way ANOVA was performed using Prism 5.0 software (****p = 0.0001, *p<0.05). Significance is comparing nonpulsed versus pulsed cells. Data is representative of two independent experiments. (B) SB cells were cultured overnight in serum free media (0.5%) containing soluble NE and P3 (10 μ g/mL) loaded with calcein-AM and then co-cultured with PR1-CTLs for 4 hours. Release of calcein-AM is indicative of cell lysis. NE and P3 pulsed cells showed increased killing versus nonpulsed SB cells. T2 cells pulsed with PR1 and CG1 or HIV peptide was used as a positive and negative control in both experiments, respectively. Cytotoxicity data are means \pm SEM from triplicate wells from 1 representative experiment.

3.2 NETs serve as a possible source of NE and P3 uptake in B-ALL cell lines

3.2.1 Identification of NET-inducing PMNs via flow cytometry

Gavillet et al. described a flow cytometry assay to identify and quantify NETs through the identification of two essential and key indicators of NETosis: histone 3 citrullination (H3Cit) and MPO. H3Cit describes the conversion of arginine to citrulline on histone tails and promotes chromatin decondensation, a key process in early NETosis. After histone decondensation, NE and MPO drive nuclear membrane rupture after recruitment to the nucleus. The latter marker is used in identifying PMNs undergoing NETosis. This is a protocol that is observer-independent and allows quantification of PMNs that will undergo NETosis. The gating strategy used included (i) identifying DAPI+ cells, (ii) H3Cit+ cells and (iii) MPO+ cells. Therefore, triple positive cells were considered PMNs undergoing NETosis⁴⁸.

PMNs isolated from a healthy buffy coat were treated with both PMA (100 nM) and Ionomycin (4 μ M) as previously described⁴⁸, and incubated for four hours at 37 °C with 5% CO₂ in air. After incubation, cells were fixed in 2% formaldehyde, blocked and incubated with primary anti-histone H3Cit Ab, AF647-conjugated secondary Ab, and anti-MPO-FITC Ab, sequentially. After staining, cells were resuspended in Hoechst 33342, trihydrochloride trihydrate and analyzed via flow cytometry. Data showed that both PMA and ionomycin induce NET formation as indicated by the shift in H3Cit and MPO expression compared to nontreated PMNs (Figure 11). However, treatment with ionomycin induced a greater population of NETosing PMNs indicated by a higher H3

Cit+ population (Figure 11). Therefore, ionomycin was used for inducing NETosis in the subsequent studies.

3.2.2 Identification of NET-inducing PMNs via confocal microscopy

In order to confirm that triple positive cells identified by flow cytometry were indeed NETosing PMNs, NETosing PMNs were stained with other NETosis markers, including DNA, NE, MPO, and P3, and identified via confocal microscopy. PMNs isolated from a healthy buffy coat were treated with ionomycin (4 μ M) and incubated for four hours at 37 °C and 5% CO₂. Cells were then fixed, and stained with Hoechst, anti-NE-AF647, anti-P3-AF488, and anti-MPO-AF488. Results indicated that healthy PMNs treated with Ionomycin undergo NETosis. This is evident by the presence of DNA extruded from the cell and extracellular expression of NE and MPO (Figure 12B). Confocal microscopy also confirmed that nontreated PMNs do not spontaneously undergo NETosis (Figure 12A). NE was proven very abundant in the NET structure, agreeing with published data (Figure 12B). However, P3 expression was not abundant in the NET structure but was instead intracellular (Figure 12C).

3.2.3 NET-associated NE and P3 are taken up by B-ALL cell lines

NETosis induces the release of neutrophil cytoplasmic granules, such as NE and P3, into the tumor microenvironment. To evaluate whether NET-associated NE and P3 are a source of uptake in B-ALL, healthy PMNs were treated with ionomycin (4 μ M) and co-cultured with B-ALL cell lines overnight. After incubation, B-ALL cell lines were stained for surface markers, as described in an earlier section, live/dead Aqua and intracellular NE and P3 uptake with anti-NE-647 and anti-P3-AF488. Notably, in overnight co-culture, such interaction

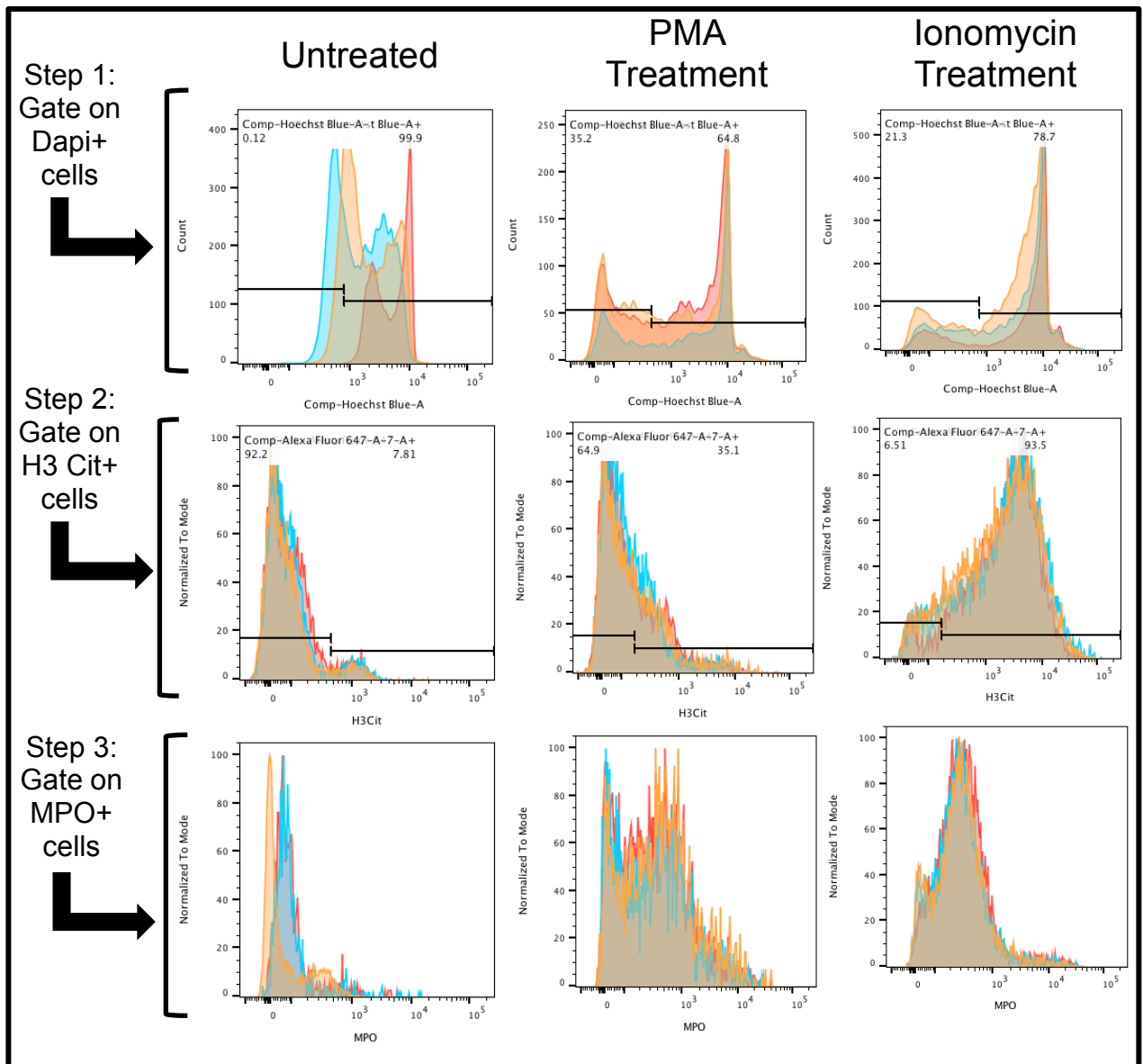


Figure 11: PMA and ionomycin induce NET formation in healthy PMNs, ionomycin at a greater extent. PMNs were isolated from a healthy donor and treated with PMA (100 nM) and ionomycin (4 μ M) for four hours at 37 $^{\circ}$ C to induce NET formation. Cells were then stained with identifying markers for early NETosis: H3 citrullination and MPO, fixed in 1% formaldehyde and stained with DAPI. Cells triple positive for DAPI, H3Cit and MPO were considered NETosing PMNs. NETs were detected in both forms of treatment. Ionomycin induced a higher population of NETs indicated by the higher percentage of H3Cit+MPO+ population.

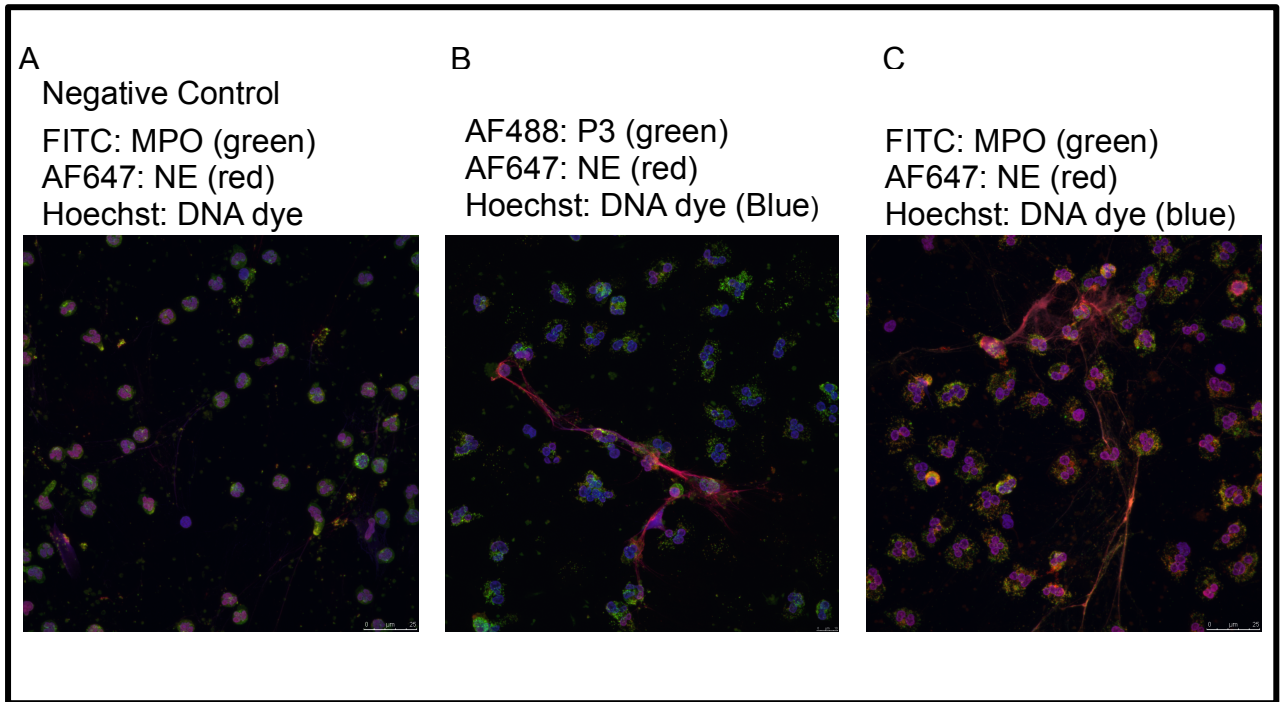


Figure 12: PMNs treated with ionomycin undergo NETosis. (A) Untreated PMNs were stained with anti-NE-AF647 (red), anti-MPO-AF488 (green) and Hoechst (blue/purple), and then imaged using confocal laser microscopy. Untreated PMNs do not appear to undergo NETosis without stimulation. Hoechst was used to stain nuclei. (B) Healthy PMNs from the same donor were stimulated with ionomycin (4 μ M) for four hours at 37 °C to induce NET formation. Samples were seeded on a cover slip, fixed in 1% formaldehyde, blocked and stained with anti-NE-AF647 (red), anti-MPO-AF488 (green), and Hoechst (blue/purple) and then imaged using confocal laser microscopy. Images indicate that PMNs stimulated with ionomycin extrude DNA and an abundance of NE (pink/purple), indicative of NETosis. (C) Samples were treated in a similar manner and stained with anti-NE-AF647 (red), anti-P3-AF488 (green) and Hoechst (purple) and then imaged using confocal microscopy. Similar to (B), when stimulated, healthy PMNs will extrude DNA and an abundance of NE (red/purple) indicative of NETosis. However, the abundance of P3 in the NET's contents is not as high as that of NE. This data agrees with published work on the abundance of granules located in NET contents.

resulted in both NE (Figure 13) and P3 (Figure 14) uptake in all four B-ALL cell lines. Flow cytometry showed that although both NET-associated and PMN-associated NE and P3 are both taken up, uptake in resting PMNs was significantly greater (Figure 6-7). Similar to uptake of soluble and PMN-associated proteases, uptake between cell lines varied greatly. Co-culturing with resting PMNs was used as a positive control as we have previously shown this to be a source of protease uptake (Figure 6-7).

Sangaletti et al proved that the integrity of the DNA backbone in the structure of NETs is necessary in maintaining the structural and functional integrity of its contents. Therefore, NETs were treated with DNase to determine the effect on uptake once granules were released from the DNA backbone. Data indicated that denaturing of the NET structure inhibited NE uptake in B-ALL cell lines (Figure 13-14), agreeing with the aforementioned study. Further, treatment with DNase showed a dose-dependent decrease in NE uptake, but did not affect P3 uptake (Figure 15). This would be expected, as NE is of much greater abundance than P3 in the NET structure.

To further prove that uptake of NET-associated NE and P3 occurred, we wanted to determine whether the treatment of ionomycin or DNase itself had any significant effect on uptake. To test this, we co-cultured all four B-ALL cell lines with irradiated PMNs (7500 cGy), and resting PMNs at a ratio of 3:1 (PMN: B-ALL), along with soluble NE and P3 (10 μ g/mL). Each treatment group was also treated with ionomycin (4 μ M) or DNase (100 U/mL) to determine if there was any effect on NE (Figure 16) and P3 (Figure 17) uptake. Data indicated that neither treatment group had any effect on uptake at any of the four conditions (Figure 16-17). Therefore, data further proved that NETs serve as a source of NE and P3 uptake, however at a lesser extent than resting PMNs.

In a previous section, we identified the uptake PMN-associated NE and P3 in B-ALL cell lines. However, to be able to properly differentiate between PMN-associated and NET-associated, it was important to determine whether resting PMNs and irradiated PMNs undergo NETosis spontaneously. To test this, we isolated PMNs from a healthy donor and stained for important early NETosis markers, H3Cit and MPO, as described in an earlier section. Cells were also stained with Hoechst, a DNA dye. Data showed that neither resting nor irradiated PMNs underwent NETosis as indicated by the negative expression of H3Cit and MPO (Figure 18).

Overall, data indicated that ionomycin and PMA induce healthy PMNs to undergo NETosis, a process that initiates NE and P3 uptake in B-ALL cell lines. It was also shown that the integrity of the NET backbone is necessary in maintaining NE uptake.

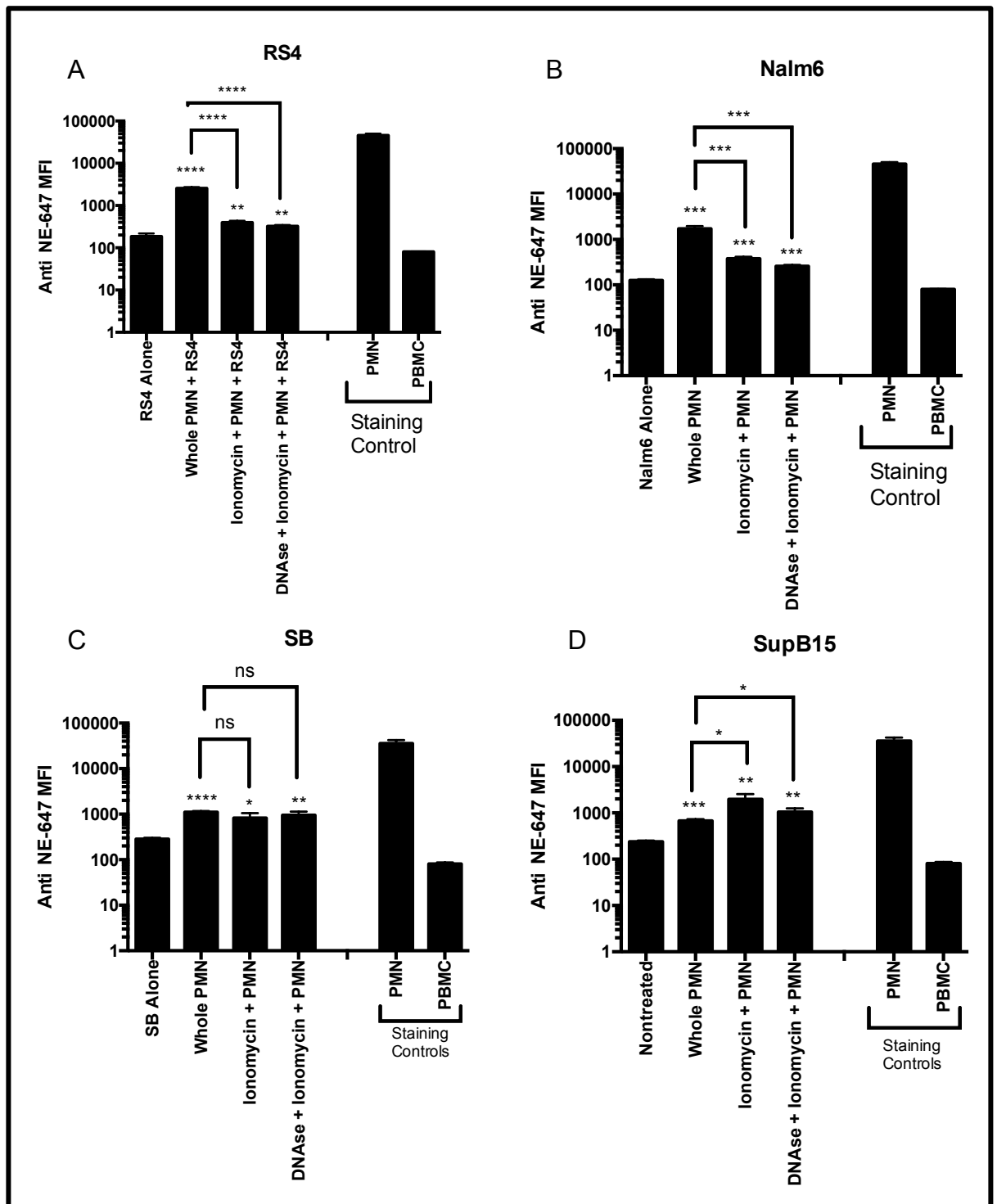


Figure 13: NET-associated NE is taken up in B-ALL cell lines. (A) RS4, (B) Nalm6, (C) SB and (D) SupB15 cell lines were co-cultured with resting PMNs, PMNs treated with ionomycin (NETs) and NETs treated with DNase overnight. After this time point, samples were surface stained with common B-ALL markers (CD10, CD19, CD34 and CD38) and live/dead Aqua, fixed in 1% formaldehyde, permeabilized in 1% solution, and stained for intracellular uptake with anti-NE-AF647. Data indicated that NET-associated NE is taken up in all four B-ALL cell lines, but at a significant lesser extent than resting PMNs. Further, treatment with DNase inhibited uptake in SupB15, Nalm6 and RS4 cell lines. PMN and PBMC stained for intracellular expression of NE and P3 were used as a positive and negative control, respectively. MFI is on the y-axis, and the axis is in log scale. A two-way ANOVA was performed using Prism 7.0 software (* $p < 0.005$)

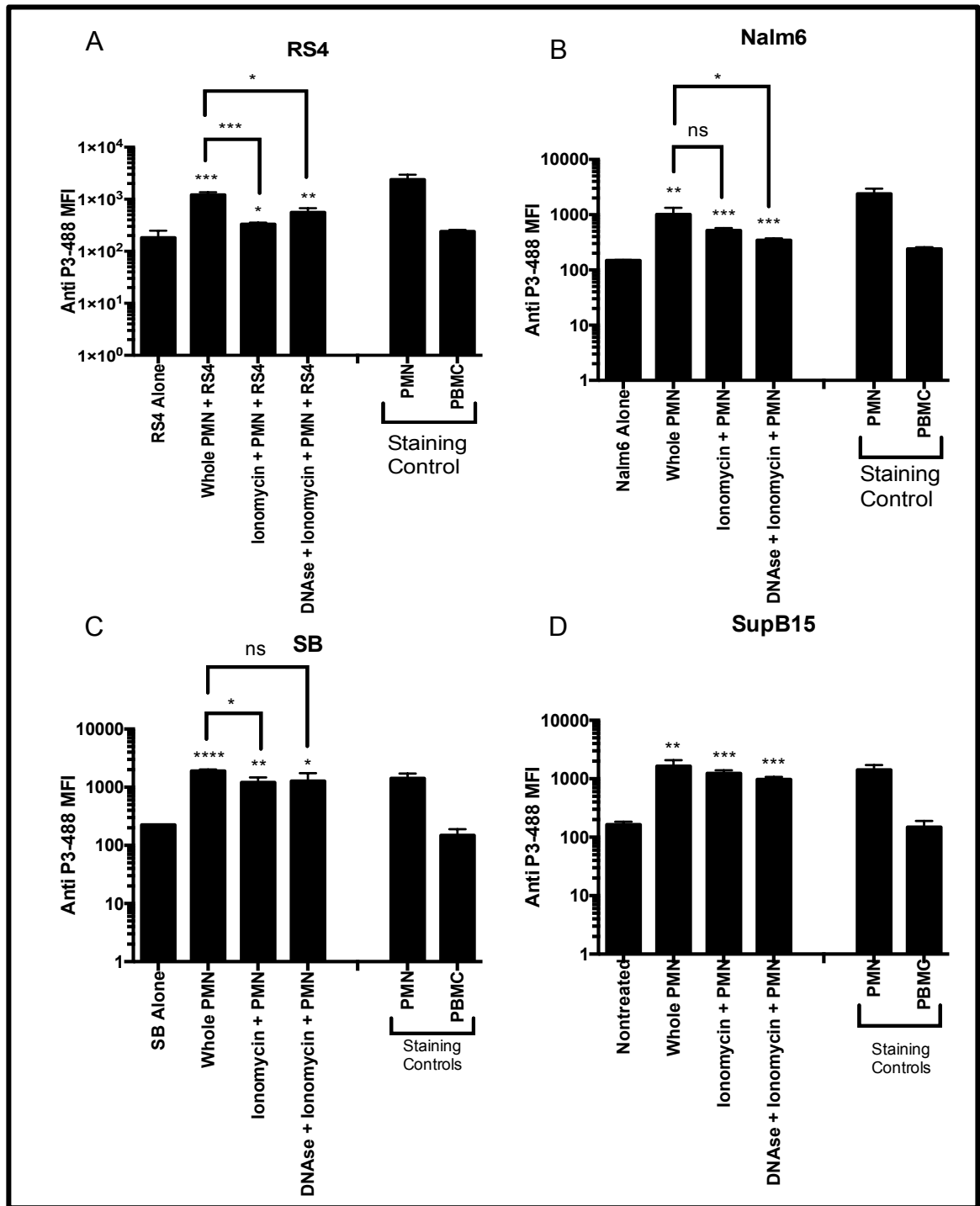


Figure 14: NET-associated P3 is taken up in B-ALL cell lines. (A) RS4, (B) Nalm6, (C) SB and (D) SupB15 cell lines were co-cultured with resting PMNs, PMNs treated with ionomycin (NETs) and NETs treated with DNase overnight. After this time point, samples were surface stained with common B-ALL markers (CD10, CD19, CD34 and CD38) and live/dead Aqua, fixed in 1% formaldehyde, permeabilized in 1% solution, and stained for intracellular uptake with anti-P3-AF488. Data indicated that NET-associated NE is taken up in all four B-ALL cell lines, but at a lesser extent than resting PMNs. Further, treatment with DNase had little effect on P3 uptake. PMN and PBMC stained for intracellular expression of NE and P3 were used a positive and negative control, respectively. MFI is expressed on the y-axis and is log scale. A two-way ANOVA was performed using Prism 7.0 software (*p<0.005).

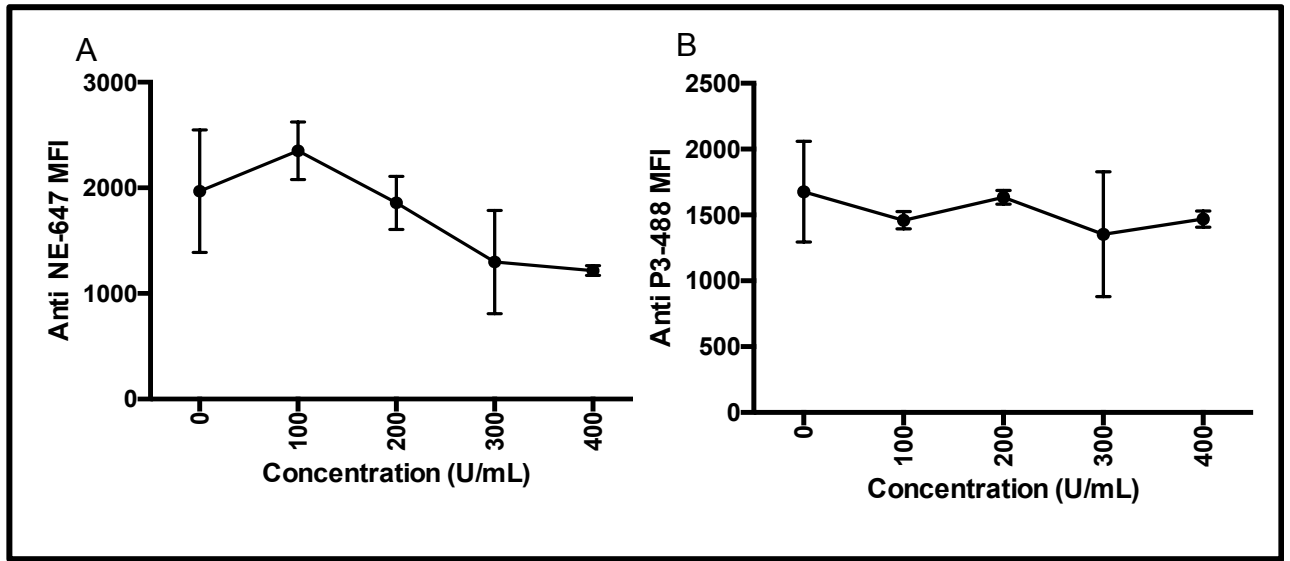


Figure 15: DNase treatment inhibits NE uptake in B-ALL cell lines in a dose-dependent manner. PMNs were isolated from a healthy donor and treated with ionomycin (4 μ M) for four hours at 37 °C to induce NETosis. After incubation period, PMNs were treated at increasing doses of DNase (0,100,200,300,400 U/mL) for 1 hour at 37 °C, and then co-cultured with B-ALL cell line overnight. At this time point, cells were stained with B-ALL phenotypic markers (CD19, CD10, CD34, CD38) and live/dead aqua, fixed in 1% formaldehyde, permeabilized in 5% perm solution, and intracellularly stained with anti-NE-AF647 and anti-P3-AF488. Data indicates that there is a dose-dependent decrease in uptake of NE (A) but no effect on P3 uptake (B). MFI is on the y-axis.

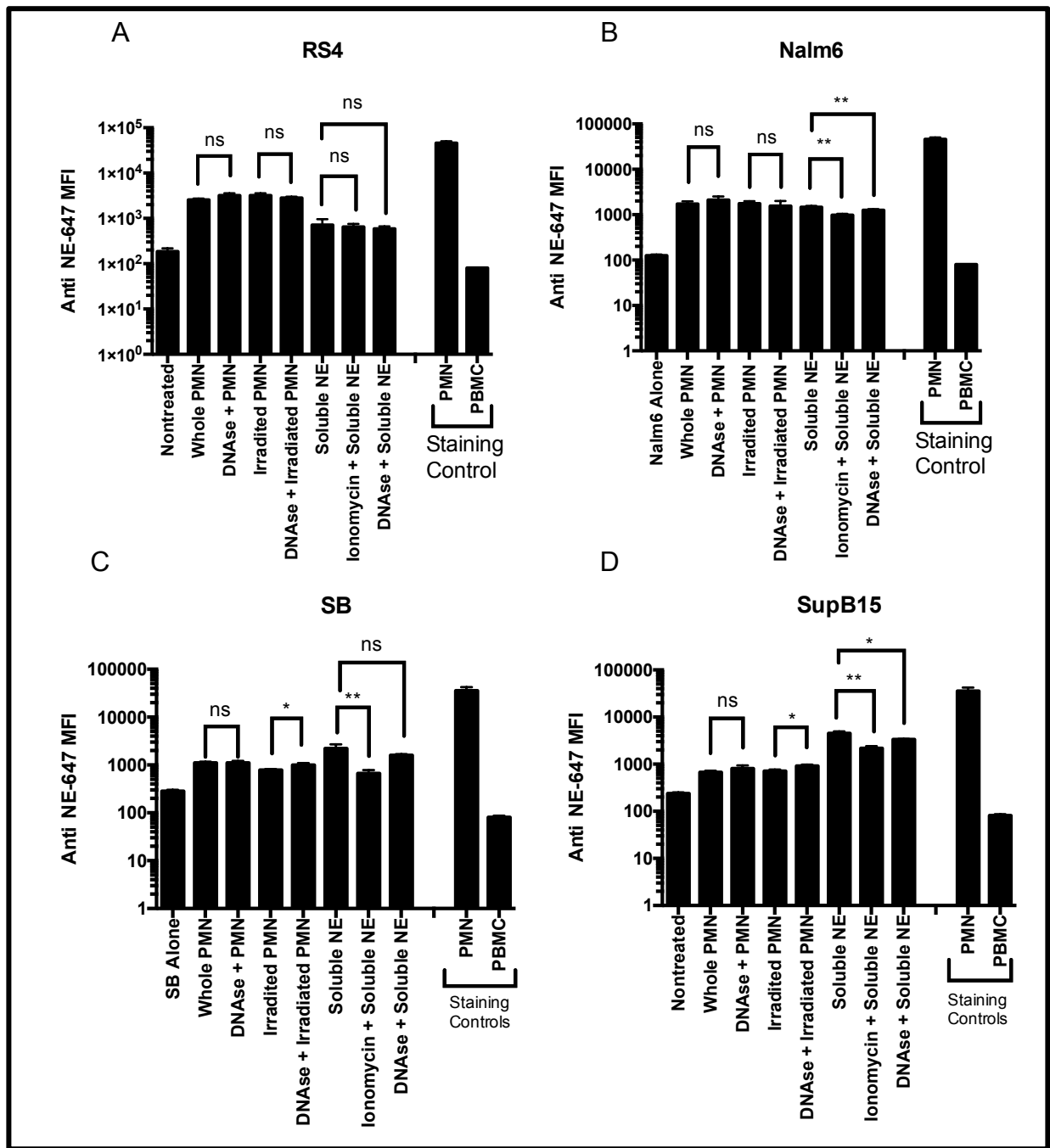


Figure 16: DNase nor ionomycin have any effect on PMN-associated NE uptake in B-ALL cell lines. (A) RS4, (B) Nalm6, (C) SB, and (D) SupB15 cell lines were co-cultured with resting PMNs, irradiated PMNs (7500 cGy), and soluble NE (10 μ g/mL). Each condition was also treated with ionomycin (4 μ M) and DNase (100 U/mL) and incubated overnight. After this time point, cells were stained for common B-ALL phenotypic markers, as previously described, fixed in 1% formaldehyde, permeabilized in 5% perm solution and stained for intracellular uptake with anti-NE-647 Ab. MFI is displayed on the y-axis and the axis is shown in log scale. Data indicated that neither ionomycin nor DNase treatment had any significant effect on PMN-associated NE uptake. Cells were analyzed by flow cytometry for intracellular uptake of NE. PMN and PBMC were used as positive and negative staining controls, respectively. A two-way ANOVA was performed using Prism 7.0 software (* $p < 0.005$).

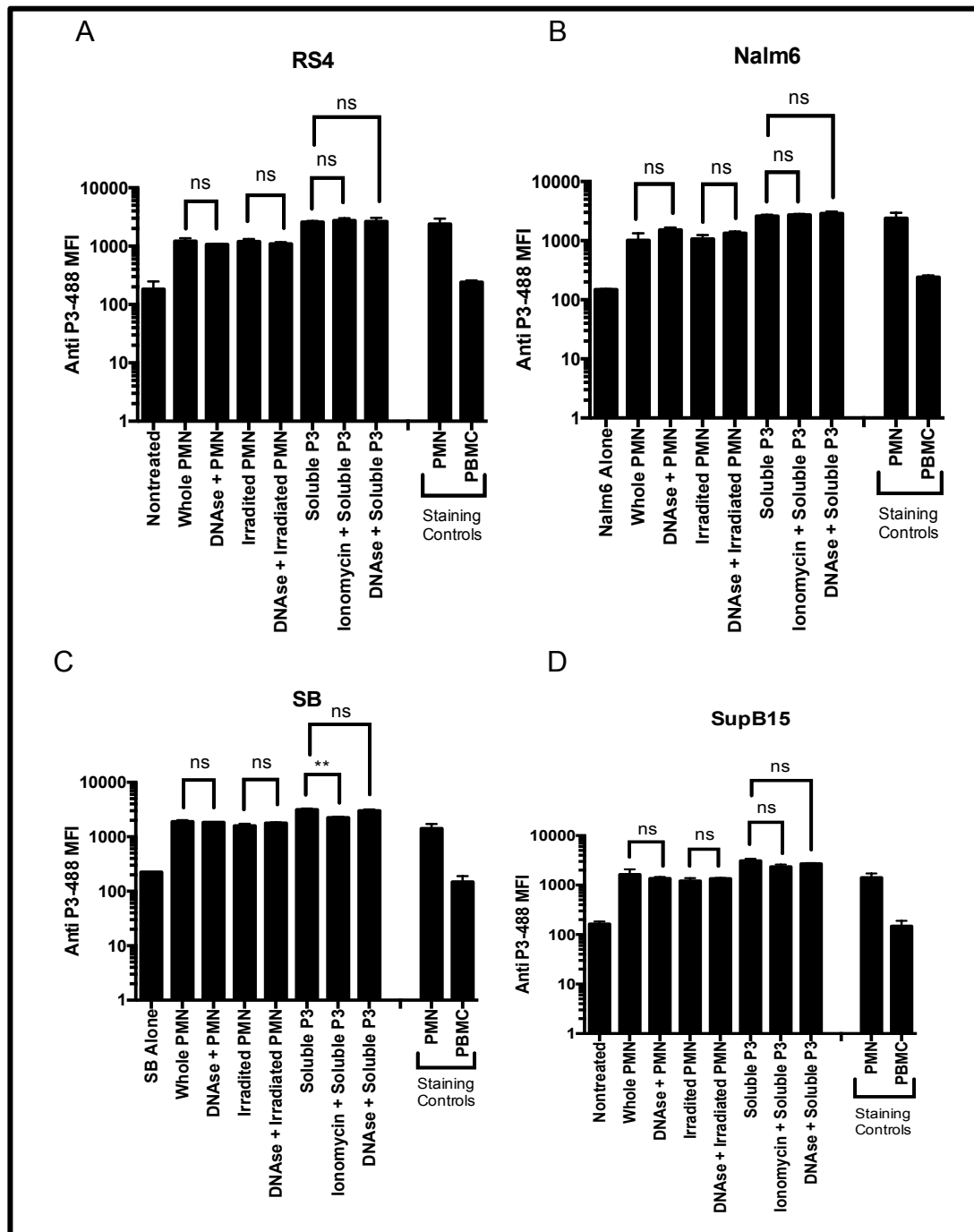


Figure 17: DNase nor ionomycin have any effect on PMN-associated P3 uptake in B-ALL cell lines. (A) RS4, (B) Nalm6, (C) SB, and (D) SupB15 cell lines were co-cultured with resting PMNs, irradiated PMNs (7500 cGy), and soluble NE (10 μ g/mL). Each condition was also treated with ionomycin (4 μ M) and DNase (100 U/mL) and incubated overnight. Similar staining protocol was performed to data showing effect on NE uptake (Figure 16). MFI is displayed on the y-axis and the axis is in log scale. Data indicated that neither ionomycin nor DNase treatment had any significant affect on PMN-associated NE uptake. Cells were analyzed by flow cytometry for intracellular uptake of NE. PMN and PBMC were used as positive and negative staining controls, respectively. A two-way ANOVA was performed using Prism 7.0 software (* $p < 0.005$).

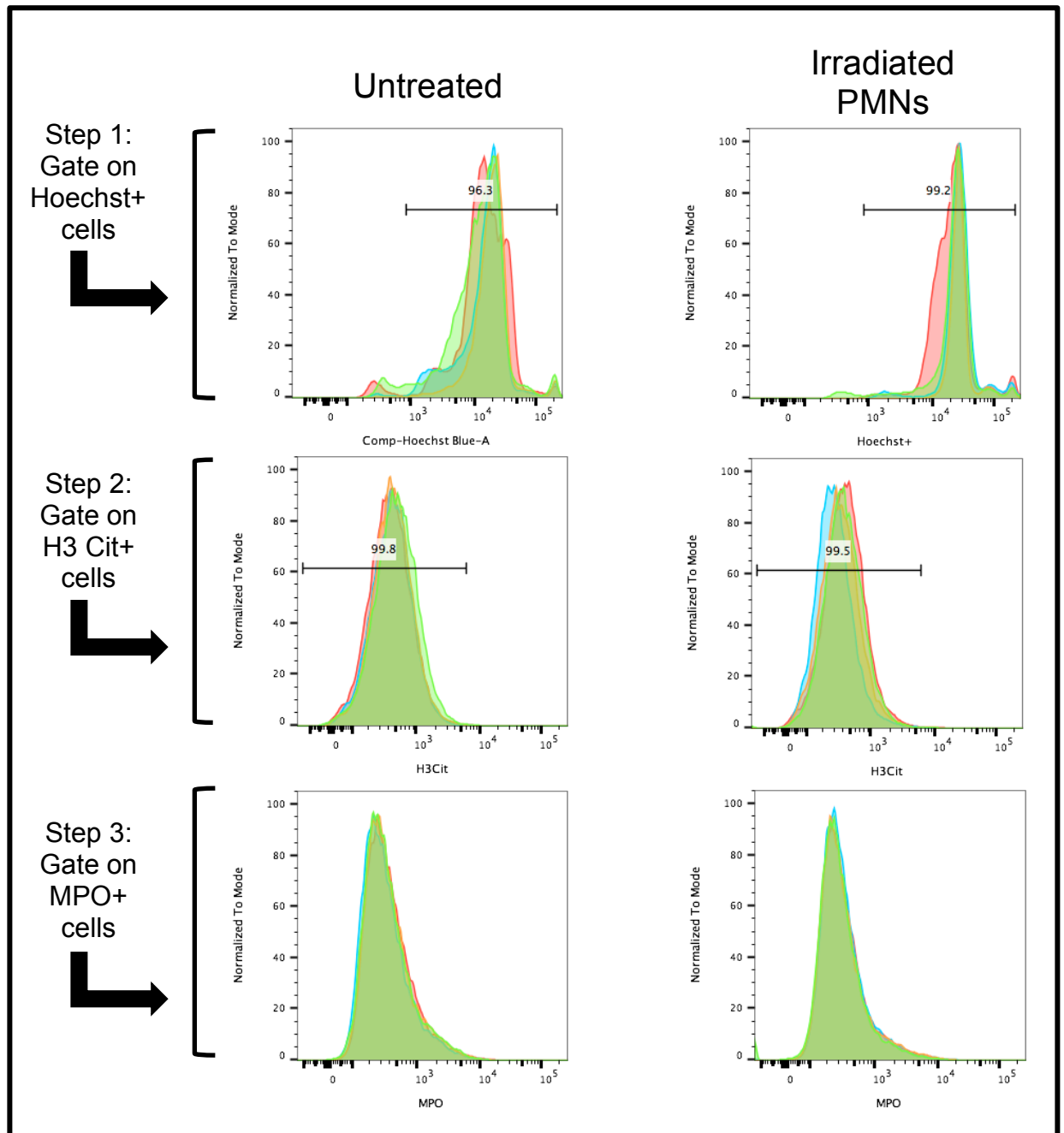


Figure 18: Resting and Irradiated PMNs do not undergo NETosis without stimulation. Resting and irradiated (7500 cGy) PMNs were stained for markers of early NETosis, H3Cit and MPO, as previously describe in an earlier section. Cells were then fixed in 1% formaldehyde, stained with Hoechst, and analyzed via flow cytometry. Gating strategy was one described earlier in identifying PMNs undergoing NETosis. Triple positive cells (Hoechst+H3Cit+MPO+) are indicative of NETosing PMNs. Data indicated that neither resting nor irradiated PMNs were positive for H3Cit or extracellular MPO. Therefore, PMNs without stimulation do not undergo spontaneous NETosis.

Chapter Four: Discussion and Future Direction

4.1 Discussion

NE and P3 are serine proteases stored in cytoplasmic azurophilic granules, and are expressed in myeloid derived cells such as granulocytes, monocytes, mast cells, and bone marrow myeloid progenitors. Both play large roles in granulocyte development in the bone marrow⁵⁰⁻⁵², and in antimicrobial defense through engulfment and degradation of foreign antigen^{13,53}. NE and P3 are found in tumors with neutrophilic and monocytic infiltration. PR1, an antigen derived from NE and P3, is overexpressed in myeloid leukemia and has been successfully targeted by PR1-targeting immunotherapies including PR1-CTLs^{17,24}, PR1 peptide vaccine²⁵, and anti-PR1/HLA-A2 (8F4) mAb^{4,5}.

The major aim of this thesis was to validate PR1 as an immunotherapeutic target in B-ALL. This was hypothesized based on data showing that APCs, including B-cells, cross-present PR1⁷. To further strengthen this hypothesis, B-ALL is located in the bone marrow, which is abundant in PMNs, and therefore NE and P3. We show in this study that B-ALL cell lines (SB, Nalm6, RS4 and SupB15), which lack endogenous NE and P3, take up soluble and PMN-associated NE and P3 (Figures 3,6,7). More importantly, we identify PR1 cross-presentation in the HLA-A2+ cell line, SB, rendering it susceptible to killing by PR1-CTLs (Figure 10). This thesis provided further evidence of a mechanism where myeloid derived antigens are taken up and cross-presented on MHC class I by malignancies that do not endogenously express NE and P3. It also further identified tumor types susceptible to killing by efficacious PR1 targeting immunotherapies.

The need to identify and develop forms of treatment that target specific antigens expressed on malignant cells is further highlighted by the relationship between the GvL effect and the toxicity and high rate of GvHD that occur after an allo-SCT. To date, many targeted immunotherapies focus on T cells specific for neo-antigens. These responses are typically to mutations in proteins that drive tumorigenesis⁵⁴. However, some tumor types, such as B-ALL, do not have many distinctive immunogenic mutations to be targeted. Therefore, identifying tumor-associated antigens, even if normal proteins, that are expressed at a higher rate on malignant cells is an important first step in targeted therapy in B-ALL.

To date, there are few antigen-specific therapies in B-ALL. Our data, however, identified PR1 as a target of interest in B-ALL. Current forms of treatment that can be utilized in targeting PR1 in B-ALL include PR1 vaccine^{1,25}, PR1-CTLs¹⁶ and 8F4 mAb^{4,5}, all efficacious in inducing lysis of malignant cells. PR1-CTLs were shown to contribute to remission in myeloid leukemia patients treated with interferon and allogeneic stem cell transplant^{17,24}. The successful killing of chronic and acute myeloid leukemia cells by PR1-CTLs supports the targeting of surface PR1 to elicit an immune response and the boosting of anti-leukemia responses. PR1 vaccine induced and enhanced leukemia-specific CD8+ T cell responses to PR1 in myeloid malignancies^{1,22,25}. The response of PR1 vaccine treatment was robust due to a higher frequency of PR1-specific CD8+ T cells with a memory phenotype in leukemia patients in comparison to healthy individuals^{17,21,23}. 8F4 mAb, engineered in our lab, was proven successful in targeting chronic and acute myeloid leukemia^{4,5} and non-myeloid malignancies including breast cancer, melanoma^{6,42} and lung cancer.⁴³ It was shown the 8F4 mediated CDC against LSCs and prevented growth of progenitor cells in

myeloid leukemia⁴. With high affinity binding to the PR1/HLA-A2 complex, it was also proven that 8F4 induced dose-dependent cytotoxicity in malignant cells but had no effect on normal hematopoietic cells⁴.

Despite data from our lab proving the anti-leukemia activity of 8F4, there are some caveats that exist in its use. For example, its inability to cross the blood brain barrier⁵. This can be worrisome in some leukemia types that spread to the brain and central nervous system. A second limitation is the expression of PR1/HLA-A2 complex on the surface of healthy B cells after NE and P3 uptake⁷. PR1/HLA-A2 surface expression on healthy B cells identified the possibility of lysis of healthy B cells with 8F4 treatment resulting in B-cell aplasia when treating B-ALL patients. Although lysis of healthy B cells is not ideal, patients can be treated with antibiotics and intravenous gamma globulin until the B cell population is no longer depleted⁵⁵. It is also important to consider the advantages of treatment despite the possibility of targeting healthy B cells. Although B-ALL patients have a high rate of response to initial therapy, 50% of patients in remission will relapse. Relapsed disease is quite aggressive and the only form of treatment in an allo-SCT, which has risks itself. Because relapse is hypothesized to be due to the growth of leukemic stem cells that are resistant to induction chemotherapy, treating with 8F4 that targets and lyses LSC is critical in enhancing the development of curative treatment in B-cell ALL.

Data in this thesis identified cross-presentation as a critical mechanism in generating an effective CTL response. Cross-presentation is a mechanism wherein exogenous antigen, such as tumor-derived antigen, is endocytosed and bound to MHC class I molecules. This process occurs in professional APCs including DCs, B cells, macrophages and neutrophils⁵⁶⁻⁵⁸, and plays an important role in eliciting immune

responses against tumor antigens. Although DCs are considered the cell most likely to cross-present due to high levels of MHC class I/II, and T cell costimulatory molecule expression, literature has verified that B cells are capable of cross-presentation as well. Heit et al showed when mice are immunized with CpG-DNA complexed with OVA, B cells are activated and capable of cross-priming OVA-specific CD8⁺ T cells⁵⁹. Following adoptive transfer of B cells that cross-present CpG-OVA, further *in vivo* work identified the priming and differentiation of naïve CD8⁺ T cells to OVA-specific CTLs. A second study identified the ability of B cells to internalize *Salmonella* after recognition and internalization via B cell receptor (BCR). *Salmonella* antigens were cross-presented in a proteasome-dependent manner on MHC class I molecules reactivating CD8⁺ memory T cells that expressed a cytotoxic phenotype, and were proven efficient in killing *Salmonella*-infected cells⁶⁰. Studies not only identified the ability of B cells to cross-present viral antigens, but self-antigens as well. Marino et al showed that B cells cross-present islet-derived autoantigens that are recognized by self-reactive CD8⁺ T cells in the pancreatic lymph node⁶¹. The result is the expansion of CD8⁺ T cells into effector cells. These studies agree with our findings identifying uptake and cross-presentation of antigens in B cells as a mechanism for inducing a robust CTL response (Figure 10) in B-ALL.

Although all aforementioned cells are capable of cross-presentation, the efficiency at which APCs take up antigen differs amongst each cell type⁶². Heit et al showed that B cells are not as efficient as DCs in antigen uptake, indicated by cellular uptake occurring in only 50% of B cells⁵⁹. This is also similar to other work done in our lab identifying the variance in NE and P3 uptake not only between cell lines, but between tumor types as well, including breast, pancreatic, melanoma, ovarian and

colon carcinomas^{6,42}. We speculate this to be due to differences in the mechanisms of protein uptake. Data from our lab indicated a dose-dependent increase in P3 uptake in breast cancer cell lines suggesting a non-receptor mediated uptake⁶. On the other hand, studies by Houghton et al showed NE was taken up by clathrin-coated vesicles, and work in our lab identified NE uptake as time and dose-dependent⁴². Both suggested NE uptake was a receptor-mediated mechanism⁴². In this study, uptake of NE and P3 plateaued after 1 hour in B-ALL cell lines (Figure 5), indicating a receptor-mediated mechanism of uptake. This suggests a difference in uptake mechanisms in tumor types, and can give reason as to why uptake in B-ALL cell lines, RS4, SupB15, SB and Nalm6, varies greatly as well (Figures 3,6-7).

Tumor cells have acquired many survival mechanisms to evade the immune system. This occurs by creating an immunosuppressive environment through cell signaling enhancement in tumor infiltrating cells⁶³, and the down-regulation of MHC and co-stimulatory surface expression. T cells specific for tumor antigen require two signals to initiate activation and expansion. The first includes the binding of the TCR to the peptide: MHC complex on the cell surface. The second is the interaction between costimulatory molecules, such as CD80 (B7-1) and CD86 (B7-2), on the surface of the APC that bind to CD28 on antigen specific T cells. Co-stimulatory signals are responsible for the cascade of signaling that occurs from the TCR⁶⁴, including cytokine secretion, T cell proliferation and effector function^{65,66}. Both TCR/MHC:peptide binding and costimulatory receptor binding are critical in eliciting an anti-tumor response. Dai et al described a phenomenon where despite high surface MHC class I and II expression, B cell-CLL was not susceptible to T cell recognition⁶⁷. Data indicated this was due to a down-regulation in co-stimulatory molecule CD86 (B7-2) on the surface of the APC⁶⁷,

inhibiting a primary immune response. Lack of CD86 expression on leukemic cells inhibits the activation of effector T cells, and instead results in T cell anergy or tolerance^{68,69}. Hematopoietic malignancies such as AML, MM and, more importantly, ALL have very low or lack CD86 expression⁷⁰⁻⁷³. In our study, down regulation of CD86 lends to the possibility that PR1 cross-presentation may lead to B-ALL tolerance. In B-ALL patients, these down regulated markers can be targeted to restore effector function of PR1-CTLs and their expansion. Some possible forms of treatment include IL-7, interferon (IFN)- γ , and IL-12 treatment. Studies have shown all three forms of treatment increase CD80 and CD86 surface expression enabling T cell recognition and function^{74,75}. This was seen in monocytes and in AML cell lines. CD8 T cell cross-priming against tumor antigens was also induced by type I IFN treatment through the stimulation of APCs^{14,76}. IFN treatment was also shown to play a role in enhancing uptake and cross-priming against soluble and cell-associated antigens. It boosts the differentiation of APCs, in this case DCs, into cells with high capacity for antigen and cross-presentation⁷⁶. A second study showed that IFN- γ elevated MHC expression and improved APC function in ALL cells⁷⁷. These forms of treatment activated both arms necessary to stimulate an immune response against tumor antigen: the ability to process and express peptide/MHC for T cell recognition and the expression of costimulatory molecules. This is important in our study because despite the capability of PR1 cross-presentation in B-ALL cells, without the expression of costimulatory molecules, treatment would prove to be ineffective, and would instead induce T cell anergy. Future work would include identifying the loss or down-regulation of costimulatory molecules, CD80 and CD86. We would then identify the effects of IL-7, IL-12 and IFN- γ treatment in eliciting an immune response against PR1.

Further surface molecules that can modulate T cell activation include CD28 and cytotoxic T-lymphocyte antigen 4 (CTLA-4) expression on the APC surface. CD28 and CTLA-4 provide stimulatory and inhibitory effects on CTLs, respectively. CD28 facilitates a T cell response through cytokine expression by binding to its ligands, CD80 and CD86, on the surface of the APC^{66,78-81}. On the other hand, CTLA-4, an inhibitory signal, is an important negative regulator of the duration and intensity of antigen-specific T cell responses^{82,83}. This function is modulated by the competition that exists between CTLA4 and CD28 in binding B7 ligands CD80 and CD86 on the APC surface. The engagement of CTLA-4 and its ligand inhibits effector T-cell function. Tumor cells often express inhibitory ligands to selectively block antitumor immunity. Current studies identify the up regulation of CTLA4 on leukemic cells^{84,85} as a mechanism inhibiting a cytotoxic T cell response. However, the design of a CTLA-4 checkpoint inhibitor, ipilimumab, proved efficacious in inhibiting CTLA-4 binding and augmenting an effector T cell response. Responses were associated with the expansion of cytotoxic CD8+ T cells, decreased activation of regulatory T cells (Tregs) and expansion of subpopulations of effector T cells in the blood⁸⁵. It would be plausible to conclude that dual treatment with CTLA-4 blockade and 8F4 mAb, treatment that induced lysis in chemotherapy resistant cells and LSCs, would be synergistic and would serve as an efficacious treatment for B-ALL patients.

Another important interaction that inhibits T cell function is between programmed death (PD)-1 and programmed death ligand (PD-L1). This interaction induces an inhibitory signal and promotes T cell apoptosis, anergy and functional exhaustion^{86,87}. T cell activation induces surface expression of PD-1, and with cytokines produced after T cell activation such as IFN- γ and IL-4, expression of PDL-1 is also induced

establishing a feedback loop in maintaining T cell function⁸⁸. In B-ALL, there is aberrant expression of PD-L1 on malignant cells⁸⁹, in addition to the surface of tumor-infiltrating macrophages and APCs in the tumor microenvironment^{90,91}. PD-L1 up regulation, similar to CTLA-4, is to hinder CTL cytotoxicity and results in T cell exhaustion. Targeted inhibition in B-ALL patients through mAb treatments may significantly affect the efficacy of T cell based immunotherapies, such as PR1-targeted therapies.

A final mechanism of immune evasion includes the down regulation of HLA class I surface expression on malignant cells, a phenomenon mainly identified in solid tumors. A recent study however identified the loss of surface HLA class I molecules on leukemic cells, specifically in relapsed patients⁹², identifying this as a mechanism by which tumor cells can evade T cell surveillance. HLA molecules expressed on the cell surface, in complex with antigen, are necessary in the recognition of tumor-specific CTLs. Often, tumor-specific antigens are intracellular proteins processed within the APC and bound to HLA class I molecules⁹². Therefore, the loss or down-regulation of HLA class I molecules would inhibit any effect of T cell based immunotherapy. The therapy presented in my thesis, for example, is PR1 specific. Its effectiveness depends completely on the HLA-A2/PR1 complex on the B-ALL cell surface. Consequently, loss or down regulation of HLA class I molecules by leukemic cells would result in a lack of PR1 cross-presentation and the ability to elicit immune response against B-ALL cells. Therefore, restoring surface expression is important in the efficacy of targeted therapy. Our study identified that co-culture with NE and P3 had no effect on HLA-A2 surface expression in any of the HLA-A2+ cell lines. However, only one of the three HLA-A2+ cell lines proved capable of cross-presentation based on PR1/HLA-A2 surface staining with anti-8F4-AF647 Ab. A possible mechanism in the inability to cross-present PR1 is

the down-regulation of HLA-A2 surface expression. SB, the cell line shown to cross-present PR1, had the highest surface expression of HLA-A2 and Nalm6 and SupB15 were at a lesser extent (Figure 9) identifying this reduction in expression a possible form of immune evasion.

As previously mentioned, cancer progression is maintained by the interaction between malignant cells and immune cells in the tumor microenvironment. Neutrophils, a white blood cell of the innate immune system, are an important cell in contributing to cancer progression through mechanisms including angiogenesis, and metastasis⁹³. One method of action in initiating metastasis is through the formation of NETs. NETosis is a unique form of neutrophil cell death, independent of apoptosis and necrosis, where chromatin and cytoplasmic granules are externalized following nuclear and cell membrane rupture. NETs play a large role in fighting bacterial infections through entrapment and degradation by NET contents, and in conditions such as atherosclerosis, diabetes and SLE^{22,94-96}. Skrzeczynska-Moncznik et al. showed that NETs modulate the link between the innate and adaptive immune response through the binding and activation of DCs via TLR9⁹⁷. This NET-mediated activation is important in the establishment of autoimmune diseases such as psoriasis, and SLE. Berger-Achituv et al. identified that NET-associated tumor antigens are taken up and displayed on DCs for activation⁹⁸. Additionally, this group showed that NETs can prime T cells through TCR signaling⁹⁸. These data support the idea that NETs can function as a danger associated molecular pattern (DAMP) to up-regulate an inflammatory response and ultimately enhance an adaptive immune response. As mentioned earlier, NETs have the ability to transfer neutrophil cytoplasmic proteins, including P3, to mDCs resulting in cross-presentation that triggers an adaptive immune response as indicated by ANCA

production⁴⁵. Therefore, we postulate that NET-associated P3 is more likely to function as a DAMP and reverse tolerance due to TLR9 activation and the P3 cross-presentation on DCs. Soluble P3 is more likely to invoke tolerance because it does not function as a DAMP since it is not associated with other proteins or DNA.

However, in recent years, formation of NETs has been identified in the tumor microenvironment. Most literature identified NET formation as being tumorigenic through inducing metastasis, relapse, and cancer-associated deep vein thrombosis. Cools-Lartigue et al. showed that NET structures released during infection initiate metastasis by promoting tumor cell presence in the circulation⁹⁹. Further, studies identified the correlation between NET formation and relapse in patients with metastatic colorectal cancer and Ewing sarcoma⁹⁸. However, my data hints to a possible anti-tumor characteristic of NET formation in the tumor microenvironment. NE and P3 are two neutrophilic proteases abundant in NETs. NE is required for nuclear decondensation to occur¹⁰⁰, and is the most abundant non-histone protein within the NET structure. The abundance of neutrophils in the bone marrow, the immunogenicity of NETs, and the presence of NE led us to hypothesize that NETs serve as a possible source of NE and P3 uptake in the bone marrow microenvironment. Our data demonstrated that NETs initiate the transfer of NET-associated NE and P3 to malignant cells (Figure 13-14). This could then potentially lead to PR1 cross-presentation, and allow for the use of PR1-targeting immunotherapies. This mechanism identified an anti-tumor effect of NET formation that could potentially be harnessed.

In conclusion, our results identified NE and P3 cross-presentation in B-ALL cell lines rendering them susceptible to killing by PR1-CTLs. We also identified PMN-associated NE and P3 as the most efficient source of uptake in B-ALL, but more

importantly, the ability of NETs to serve as a source of NE and P3 uptake. Because PMNs infiltrate various tumor microenvironments and sites of inflammation, and are the source of NE and P3, our findings suggest the ability of PR1-targeting immunotherapies to target lymphoid malignancies. Data also further described cross-presentation as a novel mechanism rendering tumors susceptible to therapies that target antigens not endogenously expressed.

An overall schematic is shown below identifying the three main steps in PR1 targeting in B-ALL (Figure 19). The first includes soluble, NET-associated and cell-associated NE and P3. The second includes the processing, cross-presentation and targeting of PR1. This results in step 3 which is tumor cell lysis.

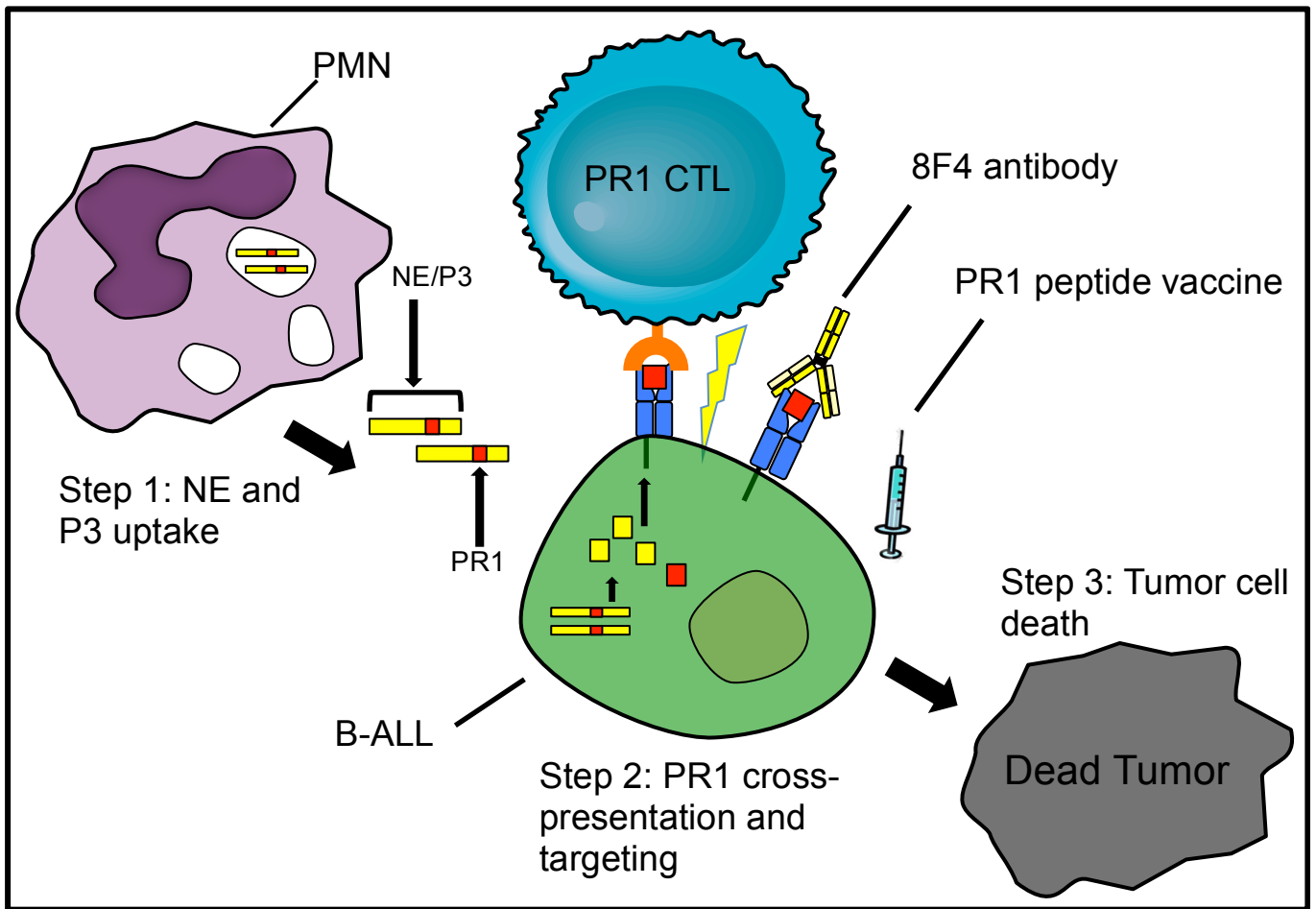


Figure 19: Proposed model of uptake and cross-presentation of NE and P3 renders B-ALL cell lines susceptible to killing by PR1-CTLs, PR1-vaccine and 8F4 mAb. This schematic identifies the overall process of PR1 cross-presentation. The first step includes the uptake of soluble, NET-associated or cell-associated NE and P3. This then leads to PR1 cross-presentation and targeting by PR1-CTLs, PR1 vaccine and 8F4 mAb. This targeting then leads to step 3, which includes tumor cell lysis.

4.2 Future Directions

The data presented in this thesis identified the ability of B-ALL cell lines to cross-present PR1; a peptide derived from serine proteases NE and P3, rendering them susceptible to killing by PR1-CTLs. Although data has shown uptake, the ability to cross-present varies among the cell lines. It would be important to determine whether uptake is receptor mediated, and if so, what antigen presentation machinery components are involved in PR1 cross-presentation in B-ALL. This would include treatment with proteasome and ER/Golgi inhibitors, and type I IFNs on PR1 cross-presentation. Treatment would include brefeldin A, which inhibits ER to Golgi transport and lactacystin, which is a proteasome inhibitor. Both are aspects of classical antigen presentation. Identifying the mechanisms involved in uptake can differentiate between cell lines that cross-present PR1 and those that do not. It would also be important to identify the expression of costimulatory molecules, such as CD86, and inhibitory receptors, including CTLA-4, on B-ALL cell lines and patient samples. As previously mentioned, both can have an effect on eliciting a T cell response against tumor antigen.

As previously mentioned, our data has proven B-ALL susceptible to killing by PR1-CTLs. We would also determine the susceptibility to 8F4 lysis *in vitro*. Further, if PR1 cross-presentation occurs rendering B-ALL susceptible to killing by 8F4, it would be necessary to determine the mechanism of action of human 8F4 against B-ALL. As mentioned earlier, previous data indicated mouse 8F4 induced cell lysis by CDC^{4,5}. To achieve this aim, we would conduct an annexin V apoptosis assay, as previously described¹⁰¹, in addition to determining if cell lysis is mediated by antibody dependent cytotoxicity assay (ADCC).

This would be initial work prior to identifying the effects of 8F4 on eliminating human B-ALL *in vivo*. *In vivo* work would include B-ALL cell lines injected into NSG mice via tail vein injections. Engraftment would be confirmed each week through blood drawings and tested for common B-ALL markers by flow cytometry. Once engraftment is confirmed, mice would be injected with 8F4 at increased doses based on conditions previously determined using AML *in vivo* NSG mouse studies⁴. Control groups would include nontreated and isotype control groups. The effect of 8F4 would be determined by blood draws and phenotyping for common B-ALL markers using flow cytometry, as previously mentioned.

Although these findings are interesting, more importantly we need to identify the presence of PR1/HLA-A2 and PR1-CTLs in B-ALL patient samples. Because B-ALL is located within the bone marrow, a site abundant in PMNs and NE and P3, and studies identified B-cells capable of PR1 cross-presentation, we expect the presence of PR1/HLA-A2 surface expression in malignant cells and more importantly the presence of PR1-CTLs in the bone marrow. We also expect these results as we have shown B-ALL cell line, SB, susceptibility to killing by PR1-CTLs. If cross-presentation was not seen in patients as we have shown in cell lines, this can be attributed to the heterogeneity of ALL cells. Further, PR1 can still be targeted by another phenomenon termed cross-dressing if PR1 cross-presentation was not evident. This is a mechanism that involves the transfer of peptide/MHC-class I complex on the surface to APCs without the need for processing. In this case, the transfer from neutrophils with PR1/HLA-A2 surface expression to malignant cells. The mechanism speculated to be involved is trogocytosis, a process that where cell-surface proteins are rapidly transferred when tumor cells are in contact with necrotic cells.

We also have yet to determine the activity of PR1 targeting therapies against primary B-ALL versus healthy B cells. In identifying the ability of healthy B-cells to cross-present PR1, we would also determine the difference in surface expression between malignant and healthy B-cells. This can identify the effects of 8F4 mAb treatment and whether it would induce lysis of healthy B cells. If PR1/HLA-A2 were expressed on normal hematopoietic stem cell (HSC) and LSC and because 8F4 eliminates LSCs, it would also be important to determine the effects of 8F4 on normal hematopoiesis. If an effect was seen in healthy B cells, we would need to identify methods of action in treating patients if B cell depletion occurs following 8F4 treatment.

Our study also identified NETs as a novel source of NE and P3 uptake in B-ALL cell lines. Future studies include first identifying the existence of NETs in the B-ALL microenvironment. Because it has been shown that only a fraction of neutrophils are capable of forming NETs, we will also need to identify whether neutrophils in the bone marrow are capable of NETosis surrounded by malignant cells and their stimuli. It would also be important to determine the balance between pro- and anti-tumor effects of NETs produced in the B-ALL microenvironment. Because most studies on NETs in the tumor microenvironment indicate pro-tumor effects including metastasis and thrombosis, identifying the balance that exists between pro- and anti-tumor effects can be important. If we would be able to harness the anti-tumor effects and up regulate NETosis and NE and P3 uptake, then lysis of malignant cells by PR1-targeting therapies can also be increased.

Because there are various mechanisms for transfer of tumor antigen to APCs for cross-presentation, there may exist various forms in the B-ALL microenvironment that lead to NE and P3 uptake. One possible example includes the secretion of exosomes

from neutrophils in the bone marrow to be endocytosed by the malignant cell. Exosomes released into the microenvironment have the ability to induce immune response, cell migration, cell differentiation and various aspects of cell-to-cell communication¹⁰². Recent studies have identified the ability of B-ALL cell to take up exosomes secreted from stromal cells in the microenvironment¹⁰³. Therefore, we expect B-ALL cells in the microenvironment to be capable of taking up secreted neutrophilic exosomes. Further studies would first include isolating exosomes secreted from healthy PMNs and identifying the presence of NE and P3 in secreted vesicles. If both are present, it would then be determined whether malignant cells can take them up. However, uptake does not mean that NE and P3 would be processed for cross-presentation to occur. We would therefore identify the mechanisms of processing and whether this would lead to antigen presentation.

These findings provide evidence that PR1 would be an effective target in treatment of B-ALL patients. Further, identifying the source of NE and P3 uptake in the bone marrow microenvironment would be beneficial in understanding and enhancing NE and P3 uptake. Data further expanded the use of 8F4 in non-myeloid tumor types, and identified cross-presentation as the mechanism rendering them susceptible.

References

1. Qazilbash, M.H., Wieder, E., Thall, P.F., Wang, X., Rios, R., Lu, S., Kanodia, S., Ruisaard, K.E., Giral, S.A., Estey, E.H., Cortes, J., Komanduri, K.V., Clise-Dwyer, K., Alatrash, G., Ma, Q., Champlin, R.E. & Molldrem, J.J. PR1 peptide vaccine induces specific immunity with clinical responses in myeloid malignancies. *Leukemia* (2016).
2. Ma, Q., Wang, C., Jones, D., Quintanilla, K.E., Li, D., Wang, Y., Wieder, E.D., Clise-Dwyer, K., Alatrash, G., Mj, Y., Munsell, M.F., Lu, S., Qazilbash, M.H. & Molldrem, J.J. Adoptive transfer of PR1 cytotoxic T lymphocytes associated with reduced leukemia burden in a mouse acute myeloid leukemia xenograft model. *Cytotherapy* **12**, 1056-1062 (2010).
3. St John, L.S., Wan, L., He, H., Garber, H.R., Clise-Dwyer, K., Alatrash, G., Rezvani, K., Shpall, E.J., Bollard, C.M., Ma, Q. & Molldrem, J.J. PR1-specific cytotoxic T lymphocytes are relatively frequent in umbilical cord blood and can be effectively expanded to target myeloid leukemia. *Cytotherapy* **18**, 995-1001 (2016).
4. Sergeeva, A., Alatrash, G., He, H., Ruisaard, K., Lu, S., Wygant, J., McIntyre, B.W., Ma, Q., Li, D., St John, L., Clise-Dwyer, K. & Molldrem, J.J. An anti-PR1/HLA-A2 T-cell receptor-like antibody mediates complement-dependent cytotoxicity against acute myeloid leukemia progenitor cells. *Blood* **117**, 4262-4272 (2011).
5. Sergeeva, A., He, H., Ruisaard, K., St John, L., Alatrash, G., Clise-Dwyer, K., Li, D., Patenia, R., Hong, R., Sukhumalchandra, P., You, M.J., Gagea, M., Ma, Q. &

- Molldrem, J.J. Activity of 8F4, a T-cell receptor-like anti-PR1/HLA-A2 antibody, against primary human AML in vivo. *Leukemia* **30**, 1475-1484 (2016).
6. Alatrash, G., Mittendorf, E.A., Sergeeva, A., Sukhumalchandra, P., Qiao, N., Zhang, M., St John, L.S., Ruusaard, K., Haugen, C.E., Al-Atrache, Z., Jakher, H., Philips, A.V., Ding, X., Chen, J.Q., Wu, Y., Patenia, R.S., Bernatchez, C., Vence, L.M., Radvanyi, L.G., Hwu, P., Clise-Dwyer, K., Ma, Q., Lu, S. & Molldrem, J.J. Broad cross-presentation of the hematopoietically derived PR1 antigen on solid tumors leads to susceptibility to PR1-targeted immunotherapy. *J Immunol* **189**, 5476-5484 (2012).
 7. Alatrash, G., Ono, Y., Sergeeva, A., Sukhumalchandra, P., Zhang, M., St John, L.S., Yang, T.H., Ruusaard, K., Armistead, P.M., Mittendorf, E.A., He, H., Qiao, N., Rodriguez-Cruz, T., Liang, S., Clise-Dwyer, K., Wieder, E.D., Lizee, G., Lu, S. & Molldrem, J.J. The role of antigen cross-presentation from leukemia blasts on immunity to the leukemia-associated antigen PR1. *J Immunother* **35**, 309-320 (2012).
 8. Zuckerman, T. & Rowe, J.M. Pathogenesis and prognostication in acute lymphoblastic leukemia. *F1000Prime Rep* **6**, 59 (2014).
 9. Chiarini, F., Lonetti, A., Evangelisti, C., Buontempo, F., Orsini, E., Evangelisti, C., Cappellini, A., Neri, L.M., McCubrey, J.A. & Martelli, A.M. Advances in understanding the acute lymphoblastic leukemia bone marrow microenvironment: From biology to therapeutic targeting. *Biochim Biophys Acta* **1863**, 449-463 (2016).
 10. Zhang, M., Sukhumalchandra, P., Enyenihi, A.A., St John, L.S., Hunsucker, S.A., Mittendorf, E.A., Sergeeva, A., Ruusaard, K., Al-Atrache, Z., Ropp, P.A.,

- Jakher, H., Rodriguez-Cruz, T., Lizee, G., Clise-Dwyer, K., Lu, S., Molldrem, J.J., Glish, G.L., Armistead, P.M. & Alatrash, G. A novel HLA-A*0201 restricted peptide derived from cathepsin G is an effective immunotherapeutic target in acute myeloid leukemia. *Clin Cancer Res* **19**, 247-257 (2013).
11. Fraser, C.J. Impact of chronic graft-versus-host disease on the health status of hematopoietic cell transplantation survivors: a report from the Bone Marrow Transplant Survivor Study. *Blood* **108**(2006).
 12. Alatrash, G. & Molldrem, J.J. Vaccines as consolidation therapy for myeloid leukemia. *Expert Rev Hematol* **4**, 37-50 (2011).
 13. Korkmaz, B., Horwitz, M.S., Jenne, D.E. & Gauthier, F. Neutrophil elastase, proteinase 3, and cathepsin G as therapeutic targets in human diseases. *Pharmacol Rev* **62**, 726-759 (2010).
 14. Le Bon, A., Etchart, N., Rossmann, C., Ashton, M., Hou, S., Gewert, D., Borrow, P. & Tough, D.F. Cross-priming of CD8⁺ T cells stimulated by virus-induced type I interferon. *Nat Immunol* **4**, 1009-1015 (2003).
 15. Molldrem, J., Dermime, S., Parker, K., Jiang, Y.Z., Mavroudis, D., Hensel, N., Fukushima, P. & Barrett, A.J. Targeted T-cell therapy for human leukemia: cytotoxic T lymphocytes specific for a peptide derived from proteinase 3 preferentially lyse human myeloid leukemia cells. *Blood* **88**, 2450-2457 (1996).
 16. Molldrem, J.J., Clave, E., Jiang, Y.Z., Mavroudis, D., Raptis, A., Hensel, N., Agarwala, V. & Barrett, A.J. Cytotoxic T lymphocytes specific for a nonpolymorphic proteinase 3 peptide preferentially inhibit chronic myeloid leukemia colony-forming units. *Blood* **90**, 2529-2534 (1997).

17. Molldrem, J.J., Lee, P.P., Wang, C., Felio, K., Kantarjian, H.M., Champlin, R.E. & Davis, M.M. Evidence that specific T lymphocytes may participate in the elimination of chronic myelogenous leukemia. *Nat Med* **6**, 1018-1023 (2000).
18. Ludewig, B., Odermatt, B., Landmann, S., Hengartner, H. & Zinkernagel, R.M. Dendritic cells induce autoimmune diabetes and maintain disease via de novo formation of local lymphoid tissue. *J Exp Med* **188**, 1493-1501 (1998).
19. Csernok, E., Ai, M., Gross, W.L., Wicklein, D., Petersen, A., Lindner, B., Lamprecht, P., Holle, J.U. & Hellmich, B. Wegener autoantigen induces maturation of dendritic cells and licenses them for Th1 priming via the protease-activated receptor-2 pathway. *Blood* **107**, 4440-4448 (2006).
20. Molldrem, J.J., Lee, P.P., Kant, S., Wieder, E., Jiang, W., Lu, S., Wang, C. & Davis, M.M. Chronic myelogenous leukemia shapes host immunity by selective deletion of high-avidity leukemia-specific T cells. *J Clin Invest* **111**, 639-647 (2003).
21. Scheibenbogen, C., Letsch, A., Thiel, E., Schmittel, A., Mailaender, V., Baerwolf, S., Nagorsen, D. & Keilholz, U. CD8 T-cell responses to Wilms tumor gene product WT1 and proteinase 3 in patients with acute myeloid leukemia. *Blood* **100**, 2132-2137 (2002).
22. Wong, S.L., Demers, M., Martinod, K., Gallant, M., Wang, Y., Goldfine, A.B., Kahn, C.R. & Wagner, D.D. Diabetes primes neutrophils to undergo NETosis, which impairs wound healing. *Nat Med* **21**, 815-819 (2015).
23. Rezvani, K., Grube, M., Brenchley, J.M., Sconocchia, G., Fujiwara, H., Price, D.A., Gostick, E., Yamada, K., Melenhorst, J., Childs, R., Hensel, N., Douek, D.C. & Barrett, A.J. Functional leukemia-associated antigen-specific memory

- CD8⁺ T cells exist in healthy individuals and in patients with chronic myelogenous leukemia before and after stem cell transplantation. *Blood* **102**, 2892-2900 (2003).
24. Kanodia, S., Wieder, E., Lu, S., Talpaz, M., Alatrash, G., Clise-Dwyer, K. & Molldrem, J.J. PR1-specific T cells are associated with unmaintained cytogenetic remission of chronic myelogenous leukemia after interferon withdrawal. *PLoS One* **5**, e11770 (2010).
 25. Rezvani, K., Yong, A.S., Mielke, S., Savani, B.N., Musse, L., Superata, J., Jafarpour, B., Boss, C. & Barrett, A.J. Leukemia-associated antigen-specific T-cell responses following combined PR1 and WT1 peptide vaccination in patients with myeloid malignancies. *Blood* **111**, 236-242 (2008).
 26. Denkberg, G., Cohen, C.J., Lev, A., Chames, P., Hoogenboom, H.R. & Reiter, Y. Direct visualization of distinct T cell epitopes derived from a melanoma tumor-associated antigen by using human recombinant antibodies with MHC- restricted T cell receptor-like specificity. *Proc Natl Acad Sci U S A* **99**, 9421-9426 (2002).
 27. Weidanz, J.A., Hawkins, O., Verma, B. & Hildebrand, W.H. TCR-like biomolecules target peptide/MHC Class I complexes on the surface of infected and cancerous cells. *Int Rev Immunol* **30**, 328-340 (2011).
 28. Reiter, Y., Di Carlo, A., Fugger, L., Engberg, J. & Pastan, I. Peptide-specific killing of antigen-presenting cells by a recombinant antibody-toxin fusion protein targeted to major histocompatibility complex/peptide class I complexes with T cell receptor-like specificity. *Proc Natl Acad Sci U S A* **94**, 4631-4636 (1997).
 29. Kumar, P., Vahedi-Faridi, A., Saenger, W., Ziegler, A. & Uchanska-Ziegler, B. Conformational changes within the HLA-A1:MAGE-A1 complex induced by

- binding of a recombinant antibody fragment with TCR-like specificity. *Protein Sci* **18**, 37-49 (2009).
30. Dao, T., Liu, C. & Scheinberg, D.A. Approaching untargetable tumor-associated antigens with antibodies. *Oncoimmunology* **2**, e24678 (2013).
 31. Davis, M.M., Boniface, J.J., Reich, Z., Lyons, D., Hampl, J., Arden, B. & Chien, Y. Ligand recognition by alpha beta T cell receptors. *Annu Rev Immunol* **16**, 523-544 (1998).
 32. Krogsgaard, M. & Davis, M.M. How T cells 'see' antigen. *Nat Immunol* **6**, 239-245 (2005).
 33. Fridlender, Z.G. & Albelda, S.M. Tumor-associated neutrophils: friend or foe? *Carcinogenesis* **33**, 949-955 (2012).
 34. Otahal, P., Hutchinson, S.C., Mylin, L.M., Tevethia, M.J., Tevethia, S.S. & Schell, T.D. Inefficient cross-presentation limits the CD8+ T cell response to a subdominant tumor antigen epitope. *J Immunol* **175**, 700-712 (2005).
 35. Francois, M., Romieu-Mourez, R., Stock-Martineau, S., Boivin, M.N., Bramson, J.L. & Galipeau, J. Mesenchymal stromal cells cross-present soluble exogenous antigens as part of their antigen-presenting cell properties. *Blood* **114**, 2632-2638 (2009).
 36. Akizuki, M., Fukutomi, T., Takasugi, M., Takahashi, S., Sato, T., Harao, M., Mizumoto, T. & Yamashita, J. Prognostic significance of immunoreactive neutrophil elastase in human breast cancer: long-term follow-up results in 313 patients. *Neoplasia* **9**, 260-264 (2007).

37. Foekens, J.A., Ries, C., Look, M.P., Gippner-Steppert, C., Klijn, J.G. & Jochum, M. The prognostic value of polymorphonuclear leukocyte elastase in patients with primary breast cancer. *Cancer Res* **63**, 337-341 (2003).
38. Yamashita, J., Ogawa, M. & Shirakusa, T. Free-form neutrophil elastase is an independent marker predicting recurrence in primary breast cancer. *J Leukoc Biol* **57**, 375-378 (1995).
39. Desmedt, C., Ouriaghli, F.E., Durbecq, V., Soree, A., Colozza, M.A., Azambuja, E., Paesmans, M., Larsimont, D., Buyse, M., Harris, A., Piccart, M., Martiat, P. & Sotiriou, C. Impact of cyclins E, neutrophil elastase and proteinase 3 expression levels on clinical outcome in primary breast cancer patients. *Int J Cancer* **119**, 2539-2545 (2006).
40. Yamashita, J.I., Ogawa, M., Ikei, S., Omachi, H., Yamashita, S.I., Saishoji, T., Nomura, K. & Sato, H. Production of immunoreactive polymorphonuclear leucocyte elastase in human breast cancer cells: possible role of polymorphonuclear leucocyte elastase in the progression of human breast cancer. *Br J Cancer* **69**, 72-76 (1994).
41. Uribe-Querol, E. & Rosales, C. Neutrophils in Cancer: Two Sides of the Same Coin. *J Immunol Res* **2015**, 983698 (2015).
42. Mittendorf, E.A., Alatrash, G., Qiao, N., Wu, Y., Sukhumalchandra, P., St John, L.S., Philips, A.V., Xiao, H., Zhang, M., Ruisaard, K., Clise-Dwyer, K., Lu, S. & Molldrem, J.J. Breast cancer cell uptake of the inflammatory mediator neutrophil elastase triggers an anticancer adaptive immune response. *Cancer Res* **72**, 3153-3162 (2012).

43. Peters, H.L., Tripathi, S.C., Kerros, C., Katayama, H., Garber, H.R., St John, L.S., Federico, L., Meraz, I.M., Roth, J.A., Sepesi, B., Majidi, M., Ruusaard, K., Clise-Dwyer, K., Roszik, J., Gibbons, D.L., Heymach, J.V., Swisher, S.G., Bernatchez, C., Alatrash, G., Hanash, S. & Molldrem, J.J. Serine Proteases Enhance Immunogenic Antigen Presentation on Lung Cancer Cells. *Cancer Immunol Res* **5**, 319-329 (2017).
44. Remijnsen, Q., Kuijpers, T.W., Wirawan, E., Lippens, S., Vandenabeele, P. & Vanden Berghe, T. Dying for a cause: NETosis, mechanisms behind an antimicrobial cell death modality. *Cell Death Differ* **18**, 581-588 (2011).
45. Sangaletti, S., Tripodo, C., Chiodoni, C., Guarnotta, C., Cappetti, B., Casalini, P., Piconese, S., Parenza, M., Guiducci, C., Vitali, C. & Colombo, M.P. Neutrophil extracellular traps mediate transfer of cytoplasmic neutrophil antigens to myeloid dendritic cells toward ANCA induction and associated autoimmunity. *Blood* **120**, 3007-3018 (2012).
46. Rodriguez-Cruz, T.G., Liu, S., Khalili, J.S., Whittington, M., Zhang, M., Overwijk, W. & Lizee, G. Natural splice variant of MHC class I cytoplasmic tail enhances dendritic cell-induced CD8⁺ T-cell responses and boosts anti-tumor immunity. *PLoS One* **6**, e22939 (2011).
47. Hosken, N.A. & Bevan, M.J. Defective presentation of endogenous antigen by a cell line expressing class I molecules. *Science* **248**, 367-370 (1990).
48. Gavillet, M., Martinod, K., Renella, R., Harris, C., Shapiro, N.I., Wagner, D.D. & Williams, D.A. Flow cytometric assay for direct quantification of neutrophil extracellular traps in blood samples. *Am J Hematol* **90**, 1155-1158 (2015).

49. Jiang, Y.Z., Mavroudis, D., Dermime, S., Hensel, N., Couriel, D., Molldrem, J. & Barrett, A.J. Alloreactive CD4⁺ T lymphocytes can exert cytotoxicity to chronic myeloid leukaemia cells processing and presenting exogenous antigen. *Br J Haematol* **93**, 606-612 (1996).
50. Bories, D., Raynal, M.C., Solomon, D.H., Darzynkiewicz, Z. & Cayre, Y.E. Down-regulation of a serine protease, myeloblastin, causes growth arrest and differentiation of promyelocytic leukemia cells. *Cell* **59**, 959-968 (1989).
51. El Ouriaghli, F., Fujiwara, H., Melenhorst, J.J., Sconocchia, G., Hensel, N. & Barrett, A.J. Neutrophil elastase enzymatically antagonizes the in vitro action of G-CSF: implications for the regulation of granulopoiesis. *Blood* **101**, 1752-1758 (2003).
52. Skold, S., Rosberg, B., Gullberg, U. & Olofsson, T. A secreted proform of neutrophil proteinase 3 regulates the proliferation of granulopoietic progenitor cells. *Blood* **93**, 849-856 (1999).
53. Kessenbrock, K., Frohlich, L., Sixt, M., Lammermann, T., Pfister, H., Bateman, A., Belaaouaj, A., Ring, J., Ollert, M., Fassler, R. & Jenne, D.E. Proteinase 3 and neutrophil elastase enhance inflammation in mice by inactivating antiinflammatory progranulin. *J Clin Invest* **118**, 2438-2447 (2008).
54. Manlove, L.S., Berquam-Vrieze, K.E., Pauken, K.E., Williams, R.T., Jenkins, M.K. & Farrar, M.A. Adaptive Immunity to Leukemia Is Inhibited by Cross-Reactive Induced Regulatory T Cells. *J Immunol* **195**, 4028-4037 (2015).
55. Davila, M.L. & Brentjens, R.J. CD19-Targeted CAR T cells as novel cancer immunotherapy for relapsed or refractory B-cell acute lymphoblastic leukemia. *Clin Adv Hematol Oncol* **14**, 802-808 (2016).

56. Beauvillain, C., Delneste, Y., Scotet, M., Peres, A., Gascan, H., Guernonprez, P., Barnaba, V. & Jeannin, P. Neutrophils efficiently cross-prime naive T cells in vivo. *Blood* **110**, 2965-2973 (2007).
57. Delamarre, L., Holcombe, H. & Mellman, I. Presentation of exogenous antigens on major histocompatibility complex (MHC) class I and MHC class II molecules is differentially regulated during dendritic cell maturation. *J Exp Med* **198**, 111-122 (2003).
58. Kovacsovics-Bankowski, M., Clark, K., Benacerraf, B. & Rock, K.L. Efficient major histocompatibility complex class I presentation of exogenous antigen upon phagocytosis by macrophages. *Proc Natl Acad Sci U S A* **90**, 4942-4946 (1993).
59. Heit, A., Huster, K.M., Schmitz, F., Schiemann, M., Busch, D.H. & Wagner, H. CpG-DNA aided cross-priming by cross-presenting B cells. *J Immunol* **172**, 1501-1507 (2004).
60. de Wit, J., Souwer, Y., Jorritsma, T., Klaasse Bos, H., ten Brinke, A., Neefjes, J. & van Ham, S.M. Antigen-specific B cells reactivate an effective cytotoxic T cell response against phagocytosed Salmonella through cross-presentation. *PLoS One* **5**, e13016 (2010).
61. Marino, E., Tan, B., Binge, L., Mackay, C.R. & Grey, S.T. B-cell cross-presentation of autologous antigen precipitates diabetes. *Diabetes* **61**, 2893-2905 (2012).
62. Fehres, C.M., Unger, W.W., Garcia-Vallejo, J.J. & van Kooyk, Y. Understanding the biology of antigen cross-presentation for the design of vaccines against cancer. *Front Immunol* **5**, 149 (2014).

63. Condeelis, J. & Pollard, J.W. Macrophages: obligate partners for tumor cell migration, invasion, and metastasis. *Cell* **124**, 263-266 (2006).
64. Boussiotis, V.A., Gribben, J.G., Freeman, G.J. & Nadler, L.M. Blockade of the CD28 co-stimulatory pathway: a means to induce tolerance. *Curr Opin Immunol* **6**, 797-807 (1994).
65. Jenkins, M.K. & Johnson, J.G. Molecules involved in T-cell costimulation. *Curr Opin Immunol* **5**, 361-367 (1993).
66. Linsley, P.S. & Ledbetter, J.A. The role of the CD28 receptor during T cell responses to antigen. *Annu Rev Immunol* **11**, 191-212 (1993).
67. Dai, Z.S., Chen, Q.F., Lu, H.Z. & Xie, Y. Defective expression and modulation of B7-2/CD86 on B cells in B cell chronic lymphocytic leukemia. *Int J Hematol* **89**, 656-663 (2009).
68. Boussiotis, V.A., Freeman, G.J., Gribben, J.G. & Nadler, L.M. The critical role of CD28 signalling in the prevention of human T-cell anergy. *Res Immunol* **146**, 140-149 (1995).
69. Gimmi, C.D., Freeman, G.J., Gribben, J.G., Gray, G. & Nadler, L.M. Human T-cell clonal anergy is induced by antigen presentation in the absence of B7 costimulation. *Proc Natl Acad Sci U S A* **90**, 6586-6590 (1993).
70. Yan, J., Ma, B., Guo, X., Sun, Y., Zhang, J. & Zhang, H. CD 80(B7-1) expression on human tumor cell lines and its costimulatory signals for T cell proliferation and cytokine production. *Chin Med J (Engl)* **111**, 269-271 (1998).
71. Zheng, Z., Takahashi, M., Aoki, S., Toba, K., Liu, A., Osman, Y., Takahashi, H., Tsukada, N., Suzuki, N., Nikkuni, K., Furukawa, T., Koike, T. & Aizawa, Y.

- Expression patterns of costimulatory molecules on cells derived from human hematological malignancies. *J Exp Clin Cancer Res* **17**, 251-258 (1998).
72. Hirano, N., Takahashi, T., Takahashi, T., Ohtake, S., Hirashima, K., Emi, N., Saito, K., Hirano, M., Shinohara, K., Takeuchi, M., Taketazu, F., Tsunoda, S., Ogura, M., Omine, M., Saito, T., Yazaki, Y., Ueda, R. & Hirai, H. Expression of costimulatory molecules in human leukemias. *Leukemia* **10**, 1168-1176 (1996).
 73. Vollmer, M., Li, L., Schmitt, A., Greiner, J., Reinhardt, P., Ringhoffer, M., Wiesneth, M., Dohner, H. & Schmitt, M. Expression of human leucocyte antigens and co-stimulatory molecules on blasts of patients with acute myeloid leukaemia. *Br J Haematol* **120**, 1000-1008 (2003).
 74. Hicks, C., Keoshkerian, E., Gaudry, L. & Lindeman, R. CD80 (B7-1) expression on human acute myeloid leukaemic cells cultured with GM-CSF, IL-3 and IL-6. *Cancer Immunol Immunother* **50**, 173-180 (2001).
 75. Buggins, A.G., Lea, N., Gaken, J., Darling, D., Farzaneh, F., Mufti, G.J. & Hirst, W.J. Effect of costimulation and the microenvironment on antigen presentation by leukemic cells. *Blood* **94**, 3479-3490 (1999).
 76. Schiavoni, G., Mattei, F. & Gabriele, L. Type I Interferons as Stimulators of DC-Mediated Cross-Priming: Impact on Anti-Tumor Response. *Front Immunol* **4**, 483 (2013).
 77. Velders, M.P., ter Horst, S.A. & Kast, W.M. Prospect for immunotherapy of acute lymphoblastic leukemia. *Leukemia* **15**, 701-706 (2001).
 78. Leach, D.R., Krummel, M.F. & Allison, J.P. Enhancement of antitumor immunity by CTLA-4 blockade. *Science* **271**, 1734-1736 (1996).

79. Chambers, C.A. & Allison, J.P. CTLA-4--the costimulatory molecule that doesn't: regulation of T-cell responses by inhibition. *Cold Spring Harb Symp Quant Biol* **64**, 303-312 (1999).
80. Lenschow, D.J., Walunas, T.L. & Bluestone, J.A. CD28/B7 system of T cell costimulation. *Annu Rev Immunol* **14**, 233-258 (1996).
81. June, C.H., Bluestone, J.A., Nadler, L.M. & Thompson, C.B. The B7 and CD28 receptor families. *Immunol Today* **15**, 321-331 (1994).
82. Salomon, B. & Bluestone, J.A. Complexities of CD28/B7: CTLA-4 costimulatory pathways in autoimmunity and transplantation. *Annu Rev Immunol* **19**, 225-252 (2001).
83. Korman, A.J., Peggs, K.S. & Allison, J.P. Checkpoint blockade in cancer immunotherapy. *Adv Immunol* **90**, 297-339 (2006).
84. Bashey, A., Medina, B., Corringham, S., Pasek, M., Carrier, E., Vrooman, L., Lowy, I., Solomon, S.R., Morris, L.E., Holland, H.K., Mason, J.R., Alyea, E.P., Soiffer, R.J. & Ball, E.D. CTLA4 blockade with ipilimumab to treat relapse of malignancy after allogeneic hematopoietic cell transplantation. *Blood* **113**, 1581-1588 (2009).
85. Davids, M.S., Kim, H.T., Bachireddy, P., Costello, C., Liguori, R., Savell, A., Lukez, A.P., Avigan, D., Chen, Y.B., McSweeney, P., LeBoeuf, N.R., Rooney, M.S., Bowden, M., Zhou, C.W., Granter, S.R., Hornick, J.L., Rodig, S.J., Hirakawa, M., Severgnini, M., Hodi, F.S., Wu, C.J., Ho, V.T., Cutler, C., Koreth, J., Alyea, E.P., Antin, J.H., Armand, P., Streicher, H., Ball, E.D., Ritz, J., Bashey, A., Soiffer, R.J., Leukemia & Lymphoma Society Blood Cancer Research, P.

- Ipilimumab for Patients with Relapse after Allogeneic Transplantation. *N Engl J Med* **375**, 143-153 (2016).
86. Butte, M.J., Keir, M.E., Phamduy, T.B., Sharpe, A.H. & Freeman, G.J. Programmed death-1 ligand 1 interacts specifically with the B7-1 costimulatory molecule to inhibit T cell responses. *Immunity* **27**, 111-122 (2007).
87. Francisco, L.M., Salinas, V.H., Brown, K.E., Vanguri, V.K., Freeman, G.J., Kuchroo, V.K. & Sharpe, A.H. PD-L1 regulates the development, maintenance, and function of induced regulatory T cells. *J Exp Med* **206**, 3015-3029 (2009).
88. Shi, L., Chen, S., Yang, L. & Li, Y. The role of PD-1 and PD-L1 in T-cell immune suppression in patients with hematological malignancies. *J Hematol Oncol* **6**, 74 (2013).
89. Chen, X., Liu, S., Wang, L., Zhang, W., Ji, Y. & Ma, X. Clinical significance of B7-H1 (PD-L1) expression in human acute leukemia. *Cancer Biol Ther* **7**, 622-627 (2008).
90. Chen, Y.B., Mu, C.Y., Chen, C. & Huang, J.A. Association between single nucleotide polymorphism of PD-L1 gene and non-small cell lung cancer susceptibility in a Chinese population. *Asia Pac J Clin Oncol* **10**, e1-6 (2014).
91. Iwai, Y., Terawaki, S., Ikegawa, M., Okazaki, T. & Honjo, T. PD-1 inhibits antiviral immunity at the effector phase in the liver. *J Exp Med* **198**, 39-50 (2003).
92. Masuda, K., Hiraki, A., Fujii, N., Watanabe, T., Tanaka, M., Matsue, K., Ogama, Y., Ouchida, M., Shimizu, K., Ikeda, K. & Tanimoto, M. Loss or down-regulation of HLA class I expression at the allelic level in freshly isolated leukemic blasts. *Cancer Sci* **98**, 102-108 (2007).

93. Olsson, A.K. & Cedervall, J. NETosis in Cancer - Platelet-Neutrophil Crosstalk Promotes Tumor-Associated Pathology. *Front Immunol* **7**, 373 (2016).
94. Hakkim, A., Furnrohr, B.G., Amann, K., Laube, B., Abed, U.A., Brinkmann, V., Herrmann, M., Voll, R.E. & Zychlinsky, A. Impairment of neutrophil extracellular trap degradation is associated with lupus nephritis. *Proc Natl Acad Sci U S A* **107**, 9813-9818 (2010).
95. Al-Mayouf, S.M., Sunker, A., Abdwani, R., Arawi, S.A., Almurshedi, F., Alhashmi, N., Al Sonbul, A., Sewairi, W., Qari, A., Abdallah, E., Al-Owain, M., Al Motywee, S., Al-Rayes, H., Hashem, M., Khalak, H., Al-Jebali, L. & Alkuraya, F.S. Loss-of-function variant in DNASE1L3 causes a familial form of systemic lupus erythematosus. *Nat Genet* **43**, 1186-1188 (2011).
96. Warnatsch, A., Ioannou, M., Wang, Q. & Papayannopoulos, V. Inflammation. Neutrophil extracellular traps license macrophages for cytokine production in atherosclerosis. *Science* **349**, 316-320 (2015).
97. Skrzeczynska-Moncznik, J., Wlodarczyk, A., Zabieglo, K., Kapinska-Mrowiecka, M., Marewicz, E., Dubin, A., Potempa, J. & Cichy, J. Secretory leukocyte proteinase inhibitor-competent DNA deposits are potent stimulators of plasmacytoid dendritic cells: implication for psoriasis. *J Immunol* **189**, 1611-1617 (2012).
98. Berger-Achituv, S., Brinkmann, V., Abed, U.A., Kuhn, L.I., Ben-Ezra, J., Elhasid, R. & Zychlinsky, A. A proposed role for neutrophil extracellular traps in cancer immunoediting. *Front Immunol* **4**, 48 (2013).

99. Cools-Lartigue, J., Spicer, J., McDonald, B., Gowing, S., Chow, S., Giannias, B., Bourdeau, F., Kubes, P. & Ferri, L. Neutrophil extracellular traps sequester circulating tumor cells and promote metastasis. *J Clin Invest* (2013).
100. Papayannopoulos, V., Metzler, K.D., Hakkim, A. & Zychlinsky, A. Neutrophil elastase and myeloperoxidase regulate the formation of neutrophil extracellular traps. *J Cell Biol* **191**, 677-691 (2010).
101. Pedersen, I.M., Buhl, A.M., Klausen, P., Geisler, C.H. & Jurlander, J. The chimeric anti-CD20 antibody rituximab induces apoptosis in B-cell chronic lymphocytic leukemia cells through a p38 mitogen activated protein-kinase-dependent mechanism. *Blood* **99**, 1314-1319 (2002).
102. Vargas, A., Roux-Dalvai, F., Droit, A. & Lavoie, J.P. Neutrophil-Derived Exosomes: A New Mechanism Contributing to Airway Smooth Muscle Remodeling. *Am J Respir Cell Mol Biol* **55**, 450-461 (2016).
103. Fei, F., Joo, E.J., Tarighat, S.S., Schiffer, I., Paz, H., Fabbri, M., Abdel-Azim, H., Groffen, J. & Heisterkamp, N. B-cell precursor acute lymphoblastic leukemia and stromal cells communicate through Galectin-3. *Oncotarget* **6**, 11378-11394 (2015).

Vita

Selena Nicole Carmona was born in San Antonio, Texas on January 22, 1991. She graduated from Alamo Heights High School in 2009 in San Antonio, Texas and attended Texas A&M College Station while majoring in Chemical Engineering. In August 2014, she began at The University of Texas MD Anderson Cancer Center UTHealth Graduate School of Biomedical Sciences.